NASA Technical Memorandum 102268

On The Estimation of Jet-Induced Fountain Lift and Additional Suckdown in Hover for Two-Jet Configurations

Richard E. Kuhn, David C. Bellavia,
Victor R. Corsiglia, and Douglas A. Wardwell

August 1991

National Aeronautics and
Space Administration

NASA Technical Memorandum 102268

On The Estimation of Jet-Induced Fountain Lift and Additional Suckdown in Hover for Two-Jet Configurations

Richard E. Kuhn, STO-VL Technology, San Diego, California
David C. Bellavia, Victor R. Corsiglia, and Douglas A. Wardwell
Ames Research Center, Moffett Field, California

August 1991

National Aeronautics and
Space Administration

Ames Research Center
Moffett Field, California 94035-1000

SYMBOLS

A_j, A_{jet}	jet exit area, ft^2
B.L.	butt line, measured from model centerline, in.
C_p	pressure coefficient, $\frac{\Delta p}{T/2A_j}$
$C_{p,base}$	pressure coefficient induced in outer regions
$C_{p,max}$	maximum pressure coefficient in fountain impingement region
$C_{p,min}$	maximum negative pressure coefficient induced in suckdown region
$C_{p,sj}$	average pressure coefficient induced by an equivalent single jet
$C_{p,\infty}$	Average pressure coefficient induced out of ground effect
d	jet diameter, ft
d_e	equivalent diameter of total jet area, ft
e	half-distance between jets, ft
h	height of planform above ground, ft
K_∞	factor used in calculating out-of-ground-effect lift loss
K_f	factor used in calculating fountain lift
K_{ms}	factor used in calculating pitching moment arm
K_s	factor used in calculating suckdown increment
ΔL	net induced lift, lb
ΔL_∞	jet-induced lift loss out of ground effect, lb
ΔL_f	fountain lift, lb
ΔL_s	induced suckdown, lb
$\Delta L_{s,f}$	forward jet-induced suckdown, lb

$\Delta L_{s,r}$	aft jet-induced suckdown, lb
ΔL_{sj}	lift loss induced by an equivalent single jet, lb
LIDs	lift improvement devices
ΔM_{∞}	Pitching moment increment induced out of ground effect, ft lb
ΔM	net jet-induced pitching moment, ft lb
ΔM_f	pitching moment increment due to fountain lift, ft lb
ΔM_s	pitching moment increment due to suckdown, ft lb
NPR	jet nozzle pressure ratio
Δp	jet-induced pressure, lb/ft^2
S	total planform area, ft^2
ΔS	area on which fountain pressures are felt, ft^2
S'	area forward or aft of midpoint between the jets, ft^2
S_s	area of outboard suckdown region, ft^2
S_v	area of inboard suckdown region (under vortex-like flow), ft^2
T	total jet thrust, lb
X_0	half-width of fountain impingement region, ft
X_{∞}	distance from moment reference point to center of total planform, positive forward of moment reference point, ft
X_f	distance from moment reference point to center of fountain lift, positive forward of moment reference point, ft
$X_{s,f}$	distance from moment reference point to center of forward lift loss, positive forward of moment reference point, ft
$X_{s,r}$	distance from moment reference point to center of aft lift loss, positive forward of moment reference point, ft

w/e	ratio of body half-width to half-distance between jets for configurations where the jets are outside the planform. For configurations where the jets are contained within the planform w/e = 1.0
y	half-width of planform at point midway between jets, ft

Subscripts

f	front jet or forward suckdown region
r	rear jet or aft suckdown region
calc	calculated value

ON THE ESTIMATION OF JET-INDUCED FOUNTAIN LIFT AND ADDITIONAL SUCKDOWN IN HOVER FOR TWO-JET CONFIGURATIONS

Richard E. Kuhn,* David C. Bellavia, Victor R. Corsiglia, and Douglas A. Wardwell

Ames Research Center

SUMMARY

Currently available methods for estimating the net suckdown induced on jet V/STOL aircraft hovering in ground effect are based on a correlation of available force data and are therefore limited to configurations similar to those in the data base. Experience with some of these configurations has shown that both the fountain lift and additional suckdown are overestimated but these effects cancel each other for configurations within the data base. For other configurations these effects may not cancel and the net suckdown could be grossly overestimated or underestimated. Also, present methods do not include the prediction of the pitching moments associated with the suckdown induced in ground effect.

The present study begins an attempt to develop a more logically based method for estimating the fountain lift and suckdown based on the jet-induced pressures. The present analysis is based primarily on the data from a related family of three two-jet configurations (all using the same jet spacing) and limited data from two other two-jet configurations.

This report presents the current status of the method, which includes expressions for estimating the maximum pressure induced in the fountain region, the minimum pressures induced in the suckdown regions, and the sizes of the fountain and suckdown regions. Correlating factors are developed to be used with these areas and pressures to estimate the fountain lift, the suckdown, and the related pitching moment increments.

INTRODUCTION

When the jets from a powered lift VTOL aircraft impinge on the ground, a wall jet is formed on the ground which flows radially outward from the impingement point. This wall jet entrains air and induces suction pressure on the lower surface of the aircraft, causing a download or suckdown. With multiple jets the radial wall jets flowing outward from their respective impingement points meet and form an upflow or "fountain" (fig. 1). The impingement of this fountain on the aircraft produces an upload which partially offsets the suckdown created by the entrainment action of the wall jets. Unfortunately, the fountain flow also induces a vortex-like flow between the fountain flow, as shown

*STO-VL Technology, San Diego, California.

in figure 2 (ref. 1). These vortex-like flows induce higher suction pressures between the fountain and the jets which produce an additional download.

A method for estimating the suckdown and fountain effects for multiple-jet configurations is presented in reference 2. This method is based on an empirical correlation of available force data. It has been found that it overestimates both the fountain lift and the additional suckdown. However, these effects appear to compensate each other and the estimate of the net suckdown is reasonably accurate for most configurations.

The most serious deficiency of the present method is that it does not include a method to estimate the pitching moments associated with the jet-induced lifts in ground effect.

The NASA Ames Research Center has undertaken a program to obtain a database of jet-induced lift, pitching moment, and pressure distribution data that will provide the basis for a more complete and logically based method. References 3 and 4 present the first data from that program. The present paper begins the process of developing the estimating method.

BASIS OF OLD METHOD

At the time of the development of the method of reference 2, only force test data were available. (The pressure distribution data of reference 1 existed but reference 1 was not found in the library search.) It was recognized that the fountain would generate positive or lifting pressures between the jets. Also, the force data showed that, for some multiple-jet configurations, the suckdown was greater than would be generated by an equivalent single jet. However, the mechanism that generated this additional suckdown and the distribution of the additional suction pressures were unknown.

The assumptions about the flow fields at the time of the development of reference 2, in effect included the assumption that the pressure distribution induced on a twin-jet configuration would look like that shown in the middle of figure 3(a). The method of reference 2 assumed that the net lift loss is made up of four terms, as shown at the bottom of figure 3(a.) These terms are: the base loss induced out of ground effect (refs. 5 and 6), the suckdown induced by an equivalent single jet (ref. 7), the lift increment imparted by the impingement of the fountain flow, and the additional suckdown induced by the multiple jets. Thus,

$$\frac{\Delta L}{T} = \frac{\Delta L_{\infty}}{T} + \frac{\Delta L_{sj}}{T} + \frac{\Delta L_{f}}{T} + \frac{\Delta L_{s}}{T}$$

The primary challenge in developing the method of reference 2 was to develop expressions for estimating the fountain and additional suckdown contributions. A theoretical approach to the fountain lift is presented in reference 8. Unfortunately, this theory contains constants and exponents that must be empirically evaluated. In order to evaluate these, the first assumption in reference 2 was that the additional suckdown was due to the additional entrainment area represented by the fountain and

model lower surface area as depicted in figure 3(b). A suckdown was calculated for the unfolded surface and subtracted from the increment due to multiple jets to obtain a fountain increment for use in evaluating the constant and exponent for the theory of reference 8. The values thus obtained appeared reasonable at the greater heights and these were adopted for the method. The fountain increments, thus predicted by the method derived from reference 8, were subtracted from the multi-jet increment to obtain a new additional suckdown increment. This additional suckdown increment was then correlated with the geometry of the configuration to develop the expression for estimating the additional suckdown. The method, thus derived, tends to overestimate both the fountain lift and the additional suckdown. These effects tend to cancel for configurations within the data base but not for others.

A better approach to evaluating the fountain lift and additional multi-jet suckdown would be to evaluate the pressures induced on the lower surface. Unfortunately, until the data of references 3 and 4 were obtained, only two very limited sets of pressure data of this type were available (refs. 1 and 9).

APPROACH TO REVISED METHOD

The bulk of this analysis is based on the data from reference 4 which presents lift, moment, and pressure distribution data on the three configurations shown in figure 4. (The principle dimensions of the models are presented in table 1.) These models (fig. 4) were flat plate representations of the planforms. Data were obtained through a range of heights and nozzle pressure ratios. Typical pressure distributions measured on the lower surface are presented in figures 5-7. (The inlet system used in the hot gas ingestion part of the investigation was removed when these pressure distributions were obtained.)

Limited pressures were also measured on the upper surface of the configuration and are presented in figures 5(e), 6(d), and 7(d). The downflow induced by the wall jets flowing outward from the impingement points of each jet should produce a slight positive pressure over the inner portion of the upper surface. However, these positive pressures were too small to measure with the instrumentation used. The data show that a low level of suction pressure is induced on the upper surface near the edge of the configuration as the flow is accelerated around the edge of the plate. These suction pressures tend to offset the suckdown. An integration of these pressures shows that the lift loss would be reduced by less than 0.5 percent of the thrust. The positive pressures that must be present over the inner region would tend to reduce this increment even further. The upper surface pressures were therefore ignored when integrating the pressures to obtain the fountain lift and suckdown increments used in the present analysis.

The limited data available in references 1 and 9 were also considered in developing the method. All the pressure distribution data available from reference 1 are presented in figure 2, and typical data from reference 9 are presented in figure 8.

Initially it was assumed (1) that the pressures induced on the outer regions of the planform (furthest from the jets and fountain) would asymptote to those that would be induced by an equivalent single jet, and (2) that the fountain lift could be obtained by integrating those pressures above the average level that would be induced by the equivalent single jet as depicted at the top of figure 9. However, it was found, as shown in figure 9, that close to the ground the suction pressures induced by these two-jet configurations in the outer regions are much less negative than would be induced by an equivalent single jet. This result suggests that the fountain and associated vortex-like flows between the jet and the fountain are in some way reducing the entrainment action of the outboard wall jet. Attempts to develop a simple way to relate the pressure in the outer region to the equivalent single-jet pressure were unsuccessful and it was decided to leave the increment due to an equivalent single-jet suckdown out of the method.

In its present form, the method assumes that the induced lift is made up of the base loss out of ground effect, the fountain lift, the suckdown induced forward of the fountain region, and the suckdown induced aft of the fountain region. And that the pitching moment can be estimated by summing the products of these lift increments multiplied by their respective arms. Thus,

$$\frac{\Delta L}{T} = \frac{\Delta L_\infty}{T} + \frac{\Delta L_f}{T} + \frac{\Delta L_{s,f}}{T} + \frac{\Delta L_{s,r}}{T}$$

and

$$\frac{\Delta M}{T d_e} = \frac{\Delta L_\infty}{T}\frac{X_\infty}{d_e} + \frac{\Delta L_f}{T}\frac{X_f}{d_e} + \frac{\Delta L_{s,f}}{T}\frac{X_{s,f}}{d_e} + \frac{\Delta L_{s,r}}{T}\frac{X_{s,r}}{d_e}$$

The definition of key factors and symbols and the expressions for key terms in the method are presented in figure 10. The development of expressions for each of these terms is presented in the following sections. The principal geometric parameters used in the method are presented in table 1 for each of the five configurations used in developing the method. In its present form the method is limited to configurations with two circular vertical jets.

LIFT LOSS OUT OF GROUND EFFECT

When hovering out of ground effect the jets supporting the aircraft entrain air and lower the pressure on the surface of the aircraft. The basic investigations of the out-of-ground-effect lift loss are presented in references 5 and 6. These studies covered nozzle pressure ratios up to about 2.5. The studies of references 3 and 4 extended the data base to nozzle pressure ratios up to 6 and showed that at these higher pressure ratios the reduction in induced lift loss was less than indicated by previous studies. Thus, the exponent to which the NPR is raised in the expression for estimating lift loss out of ground effect must be changed. Also, these data showed that the size of the chamber in which tests were conducted affects the results. The out-of-ground-effect lift loss was increased by testing in too small a room.

On the basis of latest data, the expression for the lift loss induced out of ground effect is given by

$$\frac{\Delta L_\infty}{T} = K_\infty \sqrt{\frac{S}{A_j}} \left(\frac{\Sigma \pi d}{d_e} \right)^{1.58} (NPR)^{-0.5}$$

where K_∞ is a factor that is a function of the size of the test cell

$K_\infty = -0.00010$ for test in open air

K_∞ = is -0.00015 for tests in the test cell of references 3 and 4

Out of ground effect, the pitching moment contribution is assumed to be given by the lift loss acting at the center of area of the configuration. Thus

$$\frac{\Delta M_\infty}{T d_e} = \frac{\Delta L_\infty}{T} \frac{X_\infty}{d_e}$$

where X_∞ is the distance from the center of area to the moment reference point. X_∞ is positive when the center of area is forward of the moment reference point

FOUNTAIN LIFT

The fountain lift, suckdown increments, and pitching moments were obtained from the data of references 1, 4, and 9 by surface integration of the pressures induced on the models. The integration of all positive pressures (above the level induced out of ground effect) provided the fountain increment and associated pitching moment and the integration of the negative pressures provided the suckdown increments. The fountain increments thus obtained are plotted against K.T. Yen's (ref. 8) height parameter in figure 11. Unfortunately, the data do not follow the trend expected but show a very nonlinear variation even on a log plot.

The extremely rapid reduction of the fountain lift at the higher heights (lower values of e/(e + h)) is probably due to the highly turbulent nature of the fountain flow. Flow visualization studies have shown that the fountain tends to "wave like a flag" and appears to have a finite height to which it can penetrate. Further examination of the data indicate that both the pressures and the width of the fountain region varied nonlinearly with height: the pressures decrease rapidly with height and the width of the positive pressure region increases slowly with height.

Width of Fountain Pressure Region

The width of the fountain region was taken as the width at which the pressure coefficient went through zero and is presented in figure 12. The width appears to be a function of the height to

jet-spacing ratio (h/e ratio) up to a height of about 1.5 times the half-spacing between the jets. At the greater heights the pressure coefficients are so small that it is difficult to determine the width with any precision. The available data indicates that the width of the fountain region can be estimated by

$$X_0/e = 0.8(S/A_j)^{-0.21}(h/e)^{0.5}(w/e)$$

The term w/e is introduced to accommodate those configurations where the jets are outside the planform, as in the configuration of reference 9. For configurations where the jets are contained within the planform the value of w/e is taken as unity (w/e = 1.0).

Maximum Fountain Impingement Pressure

The maximum impingement pressure in the fountain region is plotted against Yen's height parameter in figure 13. As noted above the fountain loses strength with height (low values of e/(e + h)) and there is probably a height at which $C_{p,max}$ goes to zero, however this height cannot be determined with any accuracy from the available data. For the present method two expressions are presented for estimating the maximum pressure in the fountain region; one for the lower height range (e/(e + h) > 0.4) and another for the higher operating heights (e/(e + h) < 0.4).

$$C_{p,max} = 8(e/d)^{-2}(S/A_j)^{-0.25}(e/(e+h))^{3.3} \quad \text{for } e/(e+h) > 0.4$$

$$C_{p,max} = 95(e/d)^{-2}(S/A_j)^{-0.25}(e/(e+h))^{6} \quad \text{for } e/(e+h) < 0.4$$

These expressions have included a term (e/d) to account for jet spacing in an attempt to incorporate the data of reference 1 and 9. It will be noted (fig. 13(b)) that the resulting expression overestimates the pressure for the configuration of reference 9 and slightly underestimates the pressure for reference 1.

Estimation of Fountain Lift

If the pressures throughout the fountain impingement region were constant and equal to the maximum, as presented in figure 13, the lift imparted would be simply the pressure increment multiplied by the area. In reality, the pressure is peaked at the center and drops off slightly toward the edge of the planform (in the direction perpendicular to a line between the jets) and rapidly decreases to zero in the direction of the jets. As depicted in figure 10 the present method assumes that the fountain lift is given by

$$\Delta L_f/T = K_f\left(\Delta S/2A_j\right)C_{p,max}$$

where ΔS is the area on which the fountain pressures are felt.

$$\Delta S = (2X_0)(2y)$$

and K_f adjusts for the fact that the maximum pressure is not constant over the entire fountain area. From figure 14:

$$K_f = 0.5$$

The fountain lift estimated by the above expression is compared with the experimental data (obtained by integrating the pressures over the fountain area) in figure 15. The comparison shown in figure 15(a) shows that the method predicts the data from which it was derived within about 1 percent of the thrust.

The method also predicts the single data point for the reference 1 configuration within about 1 percent of the thrust (fig. 15(b)). However, it overpredicts the fountain lift on the configuration of reference 9. Even when the experimental values of the fountain width and pressure are used, the fountain lift is overpredicted, indicating that the value of K_f is smaller than 0.5 for this configuration. More data on this type of configuration will be needed to provide a basis for extending the method to cover these configurations.

Estimation of Fountain Pitching Moment

The pitching moment contribution of the fountain lift of a two-jet configuration with equal thrust on both jets would be expected to be zero (the pressure distribution would be expected to be symmetrical between the jets). However, the data show that for the delta-wing and wing-body configurations the fountain is shifted aft, resulting in a small nose-down moment. Apparently, the greater suckdown experienced aft (larger suckdown area) shifts the fountain aft. The pitching moment increment due to the fountain is plotted against the fountain lift (both determined from integration of the fountain pressure distribution) in figure 16. These data indicate that the effective arm at which the fountain lift is acting can be approximated by

$$X_f/d_e = 0.2(1 - (S'_r/S'_f))$$

The increment of pitching moment due to the fountain is then given by

$$\Delta M_f/Td_e = (\Delta L_f)/T)(X_f/d_e)$$

SUCKDOWN

The wall jets flowing outward from the impingement points of the jets and the vortex-like flows between the fountain and the jets induce suction pressures over most of the lower surface. These suction pressures reach a peak under the vortex-like flows between the jets and the fountain.

In the present method the suckdown associated with the forward jet and the aft jet are estimated separately so they can be used in estimating the moments. It is assumed that the suckdown due to these pressures can be estimated by a process similar to that used for estimating the fountain lift. That is, the suckdown is the product of the minimum pressure multiplied by (1) the area involved and (2) a factor to account for the fact that the pressure is not uniform over the area involved. Thus,

$$\Delta L_s = K_s\left(C_{p,min} - C_{p,\infty}\right)(S' - \Delta S/2)/2A_j$$

Maximum Suckdown Pressure

The most negative pressures are induced adjacent to the fountain under the vortex-like flow between the fountain and the jets. Figure 17 presents the peak negative pressures as a function of Yen's height parameter. Because the lift loss induced out of ground effect is estimated (and included in the method) as a separate increment, the average pressure induced out of ground effect ($C_{p,\infty}$) has been subtracted from the pressure distributions induced in ground effect.

Figure 17 shows that the magnitude of the peak suction pressure is a function of height and the amount of surface area surrounding the jet. The data currently available indicate that the peak suction pressure can be estimated by

$$C_{p,min} - C_{p,\infty} = -0.71(e/d)^{-2}(S'/A_j)^{0.25}(e/(e+h))^{3.5}$$

This expression includes a term $(e/d)^{-2}$ which was introduced to account for jet spacing (as was included in the expression for fountain pressure) to incorporate the configurations of references 1 and 9. Figure 17(d) indicates good agreement with these data.

Estimate of Suckdown

If the pressure over the suckdown region were constant at the level of the maximum suckdown pressure, the suckdown would be simply the pressure increment multiplied by the area. In reality the pressure peaks under the vortex-like flow between the jet and the fountain and drops off rapidly toward the fountain and toward the edges of the configuration. A factor K_s is introduced to account for the nonuniform pressure distribution.

The shape factor for the fountain lift K_f was found to be a constant with a value of 0.5. For the suckdown, however, the shape factor K_s was found to be a function of several variables. It was found that that the ratio of the area under the vortex-like flow between the fountain and the jet (S_v) to the area outboard of the jet (S_s) was a primary parameter. In the present method the shape factor for the suckdown region is defined as

$$K_s = 0.1(S_v/S_s)^{0.55}(e/d)^2(NPR)^{-0.12}(h/d_e)^{exp}$$

where the exponent is defined as

$$\exp = (1.3(S_v/S_s)^{-0.25} - 1)$$

The area under the vortex-like flow between the fountain and the jet (S_v) (fig. 10) varies with height because the width of the fountain region expands with increasing height. This area is calculated by

$$S_v = S' - S_s - \Delta S/2$$

In the present method the suckdown associated with each jet is calculated separately so that it can be used in calculating the ground-effect-induced pitching moments. The estimated suckdown calculated by the above method is compared with the suckdown increments determined from integration of the pressure distributions for the three configurations of reference 4 in figure 18.

Estimation of Pitching Moments Associated with Suckdown

As indicated above, the present method assumes that the moments can be estimated by multiplying the estimated suckdown by the effective arm at which the suckdown acts. To determine the effective arm the moments are plotted against the suckdown as shown in figure 19 (both moments and suckdown were determined by integration of the appropriate pressure distribution). It was found that at the lower lift and moment combinations (greater heights—approaching out of ground effect) the effective arm was the distance from the moment reference point to the center of area aft (or forward) of the moment reference point. As the ground is approached the suckdown and moment both increase but at different rates and the effective arm is reduced. This is to be expected as the pressure distribution tends to peak under the vortex like flow between the fountain and the jet. As shown in figure 19, the factor that accounts for this reduction in the effective arm is proportional to the suckdown and is given by

$$K_{m,s} = 1 + 0.8(\Delta L_s - \Delta L_\infty)/T$$

and the pitching moment associated with each suckdown area is given by

$$(\Delta M_s - \Delta M_\infty)/Td_e = K_{m,s}((\Delta L_s - \Delta L_\infty)/T)(X/d_e)$$

COMPARISON OF ESTIMATES WITH EXPERIMENTAL DATA

Estimates made by the present method and by the method of reference 2 are compared with experimental data in figures 20-24. In general the present method does a good job of duplicating the data of reference 4, which was the primary base for its development. And it does a much better job than the method of reference 2, which overestimates both the fountain lift and the suckdown. In

addition, the present method includes expressions for predicting the pitching moments which are not available in the method of reference 2.

The present method grossly overpredicts the fountain lift and underpredicts the suckdown for the tilt-nacelle configuration of reference 9. In this configuration the jets are external to the surface on which the fountain and suckdown are induced, and the factors included in the method for this type of configuration are inadequate. The old method (ref. 2) does a better job of predicting the net suckdown for this configuration.

CONCLUSIONS

The revised method developed here for estimating the fountain lift, suckdown, net lift loss, and associated pitching moments shows that a useful method can be developed with the approach taken. It shows that, as suspected, the available method for estimating suckdown and fountain lift overestimates these terms. This study has identified the primary factors important to generating both the fountain lift and the suckdown.

However, in its present form the method is limited. It is limited to configurations having two circular jets of equal thrust issuing from flat planforms. A factor to account for the effect of jet spacing is included but is based on very limited data.

Additional pressure distribution data of the type used here should be obtained so that the method can be extended to other jet spacings of 2-, 3-, and 4-jet configurations. The data base should also be expanded to include the effects of wing height, rectangular jets, and differential thrust.

REFERENCES

1. Hall, G. R.; and Rogers, K. H.: Recirculation Effects Produced by a Pair of Heated Jets Impinging on a Ground Plane. NASA CR-1307, May 1969.

2. Kuhn, R. E.: An Engineering Method for Estimating the Induced Lift on V/STOL Aircraft Hovering In and Out of Ground Effect. NADC-80246-60, Jan. 1981.

3. Bellavia, D. C.; Wardwell, D. A.; Corsiglia, V. R.; and Kuhn, R. E.: Suckdown and Pressure Distributions Induced on Circular Plates in Ground Effect by a Single Lifting Jet. NASA TM-102816.

4. Bellavia, D. C.; Wardwell, D. A.; Corsiglia, V. R.; and Kuhn, R. E.: Suckdown, Fountain Lift and Pressure Distributions Induced on Two Jet VTOL Configurations Hovering in Ground Effect. NASA TM-102817.

5. Gentry G. L.; and Margason, R. J.: Jet-Induced Lift Losses on VTOL Configurations Hovering In and Out of Ground Effect. NASA TN D-3166, Feb. 1966.

6. Shumpert, P. K.; and Tibbetts, J. G.: Model Tests of Jet-Induced Lift Effects on VTOL Aircraft in Hover. NASA CR-1297, March 1969.

7. Wyatt, L. A.: Static Tests on Ground Effect on Planforms Fitted with a Centrally Located Round Lifting Jet. Ministry of Aviation, CP749, June 1962.

8. Yen, K. T.: On the Vertical Momentum of the Fountain Produced by Multi-Jet Vertical Impingement on a Flat Plate. NADC-79273-60, Nov. 1979.

9. Dudley, M. R.; Eshleman, J. E.; and Schell, C. J.: Full Scale Ground Effects of Twin Impinging Jets Beneath a Subsonic Tactical V/STOL Aircraft. AIAA Paper 86-2704, Oct. 1986.

Table 1. Geometric characteristics of configurations

Configuration		Delta wing	Wing-body	Body alone	Circular disc	Tilt nacelle
Reference		4	4	4	1	9
Span, width	ft	1.67	1.67	0.333	1.5	19.6
Length	ft	2.83	2.83	2.83	1.5	6.17
d	ft	0.103	0.103	0.103	0.104	3
d_e	ft	0.145	0.145	0.145	0.148	4.24
y	ft	0.480	0.544	0.166	0.75	9.8
e/d		5.98	5.98	5.98	3.5	1.94
S/A_j		155.7	105.2	50.5	104	7.4
S'_f/A_j		41.2	33	23	52	3.7
S'_r/A_j		114	72	27	52	3.7
$S_{s,f}/A_j$		13.3	10.8	10.8	—	—
$S_{s,r}/A_j$		71.1	15.8	15	—	—
w/e		1	1	1	1	0.527
X_f/d_e		2.93	3.08	3.96	—	—
X_r/d_e		–5.39	–3.25	–4.67	—	—
X_∞/d_e		–3.66	–1.71	–0.72	—	—

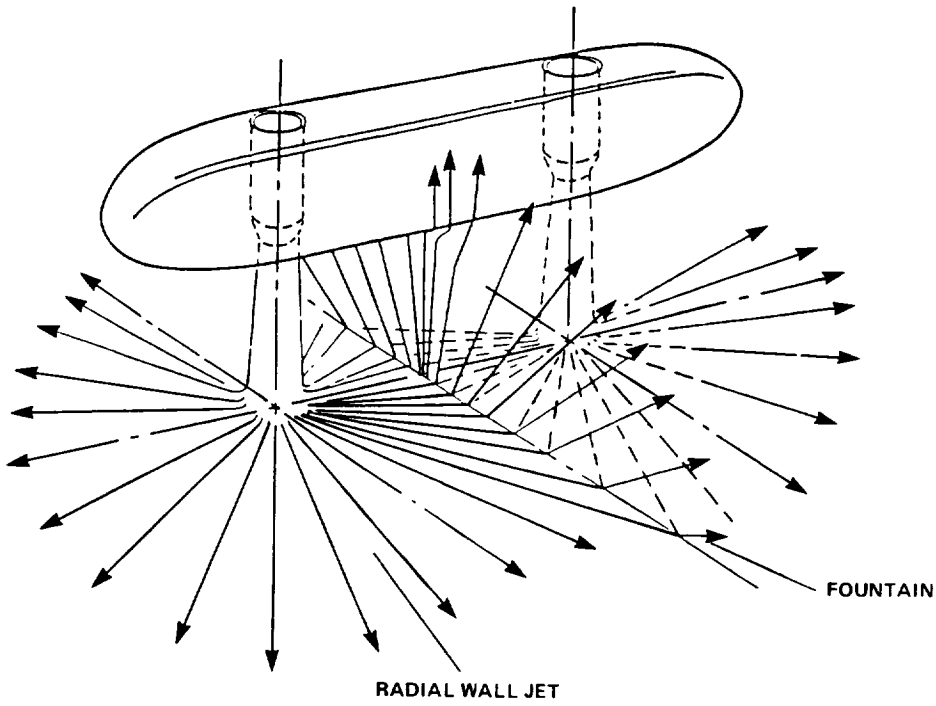

Figure 1. Fountain flow generated between a pair of jets.

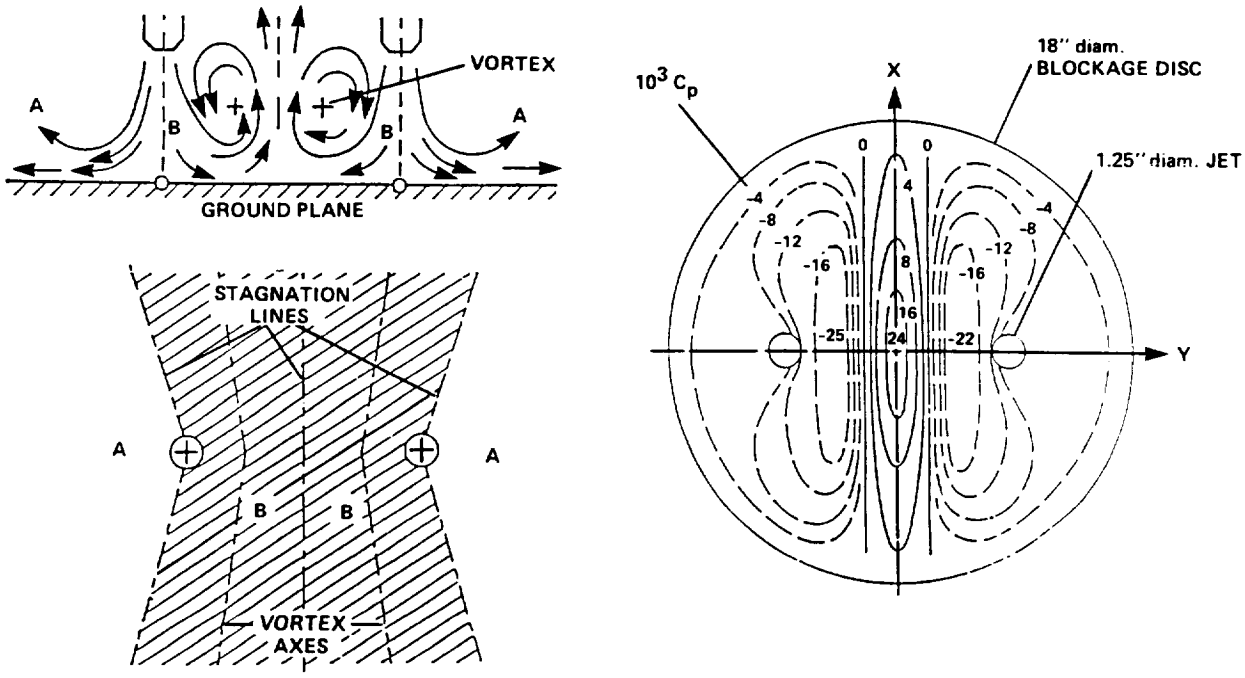

Figure 2. Flow field and induced pressures observed in reference 1.

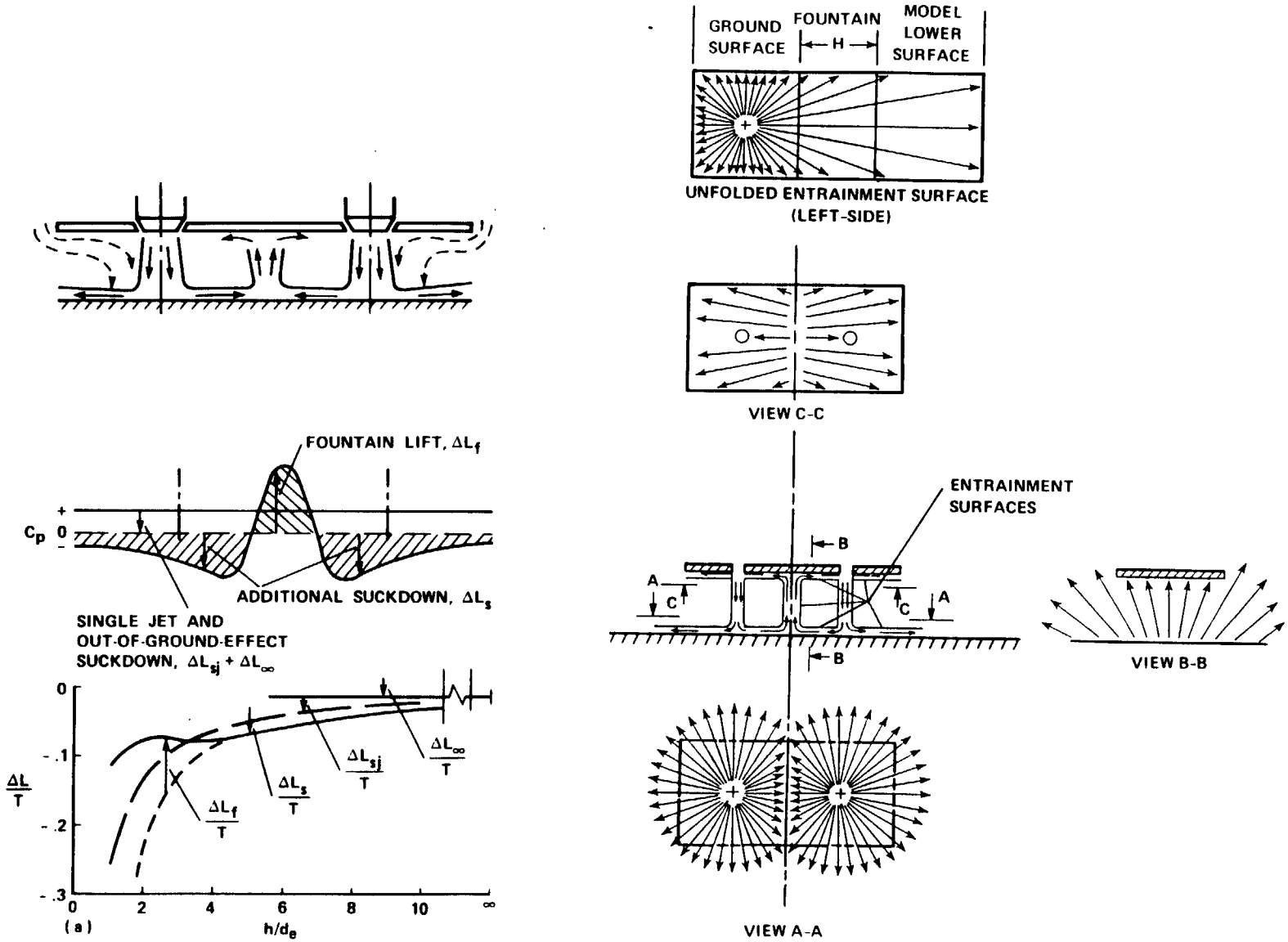

a) Increments making up induced lift loss. b) Flow field assumed in reference 2 for estimating additional suckdown.

Figure 3. Basis of method of reference 2.

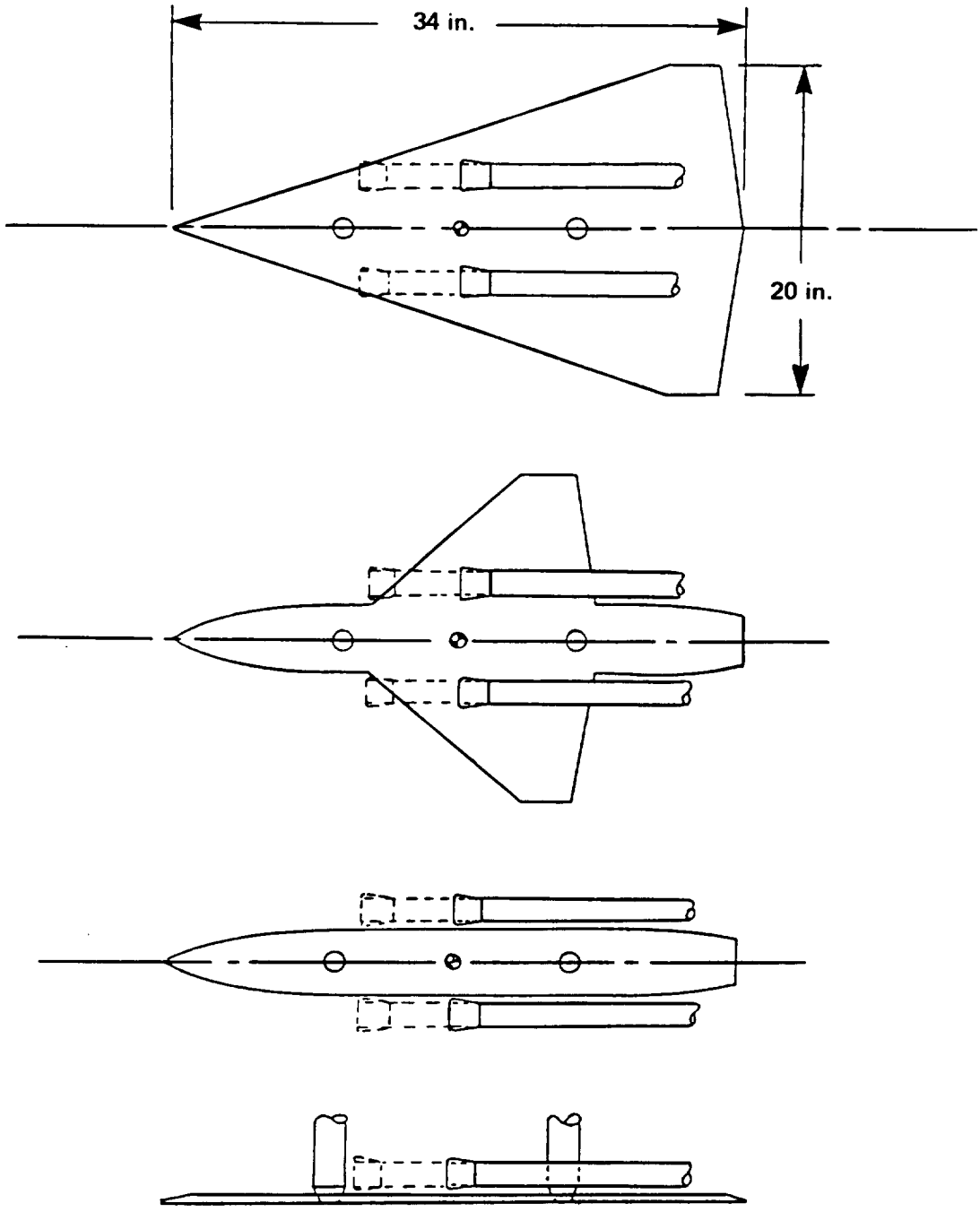

Figure 4. Configurations used in the investigation of reference 4.

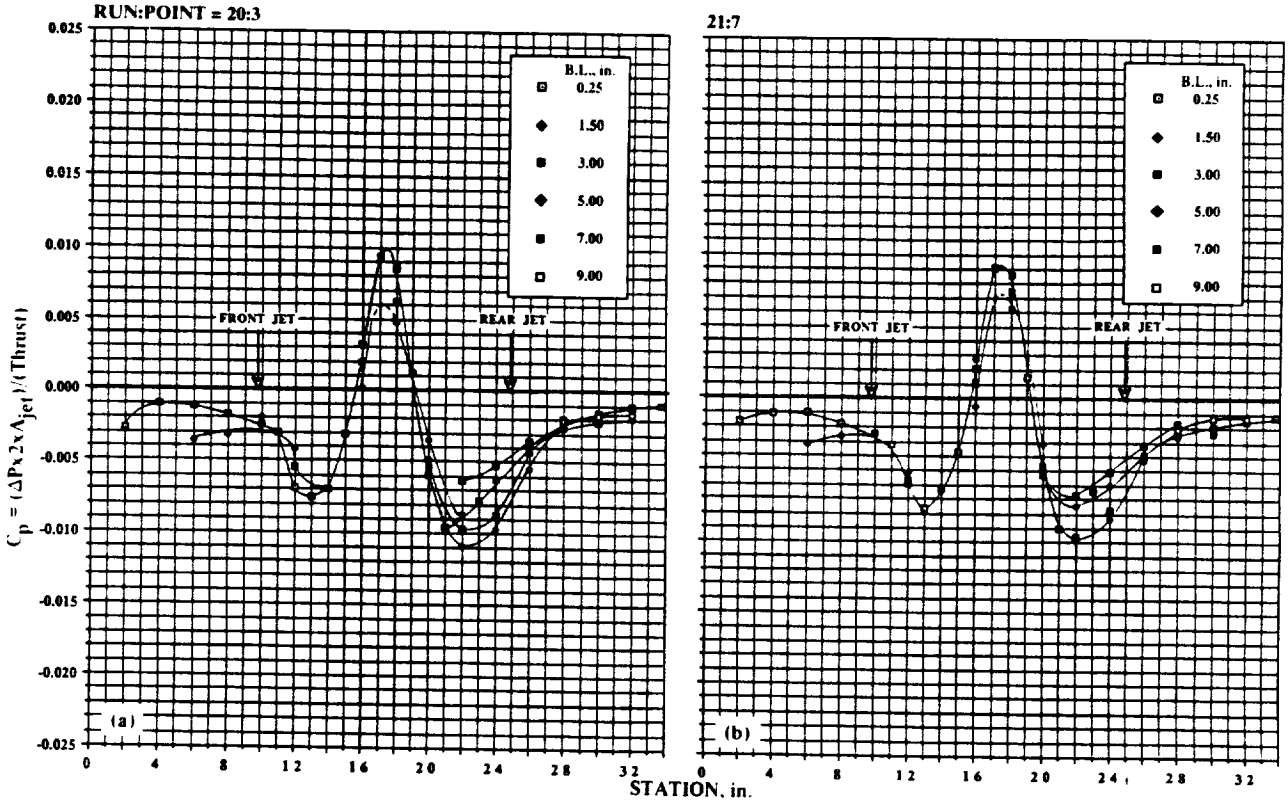

a) Lower surface pressure, NPR = 2. b) Lower surface pressures, NPR = 3.

Figure 5. Typical pressure distribution from the delta wing configuration of reference 4. h/de = 3.5.

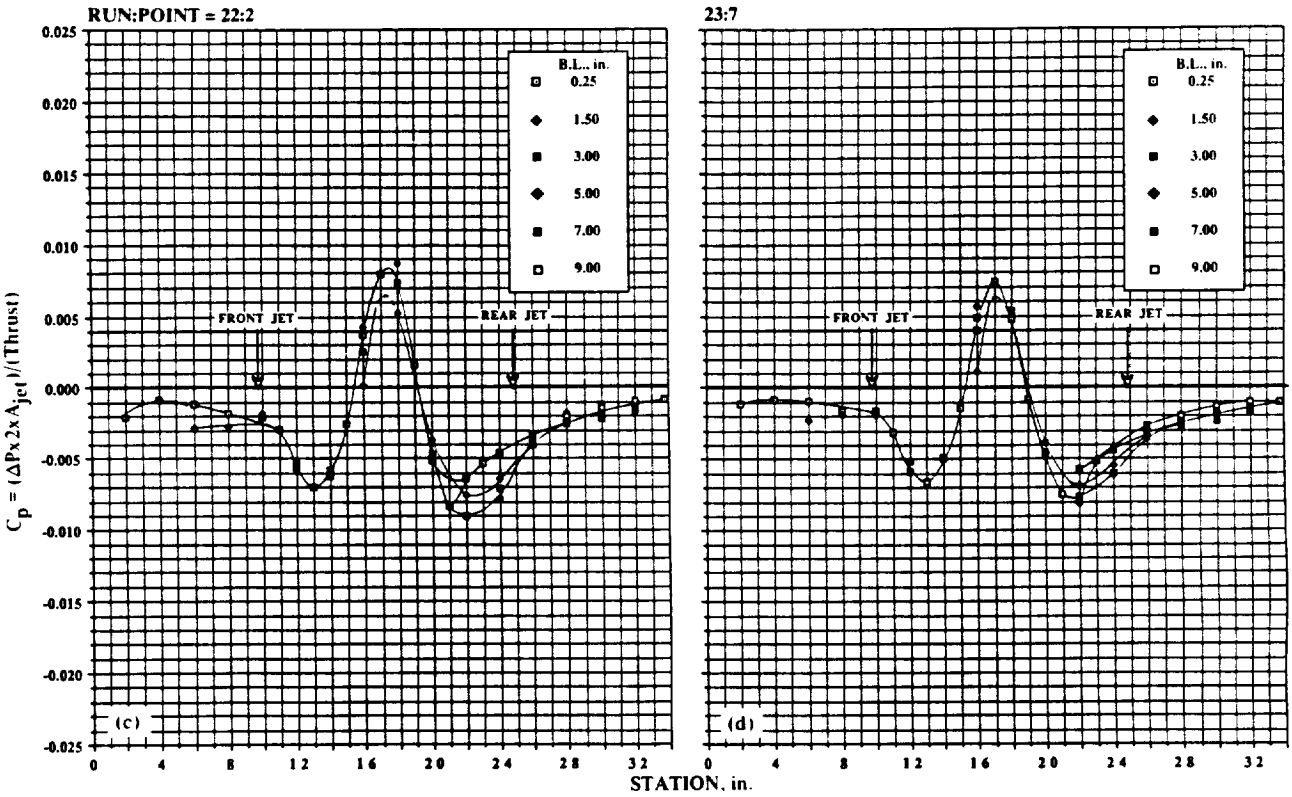

c) Lower surface pressures, NPR = 4. d) Lower surface pressures, NPR = 5.

Figure 5. Continued.

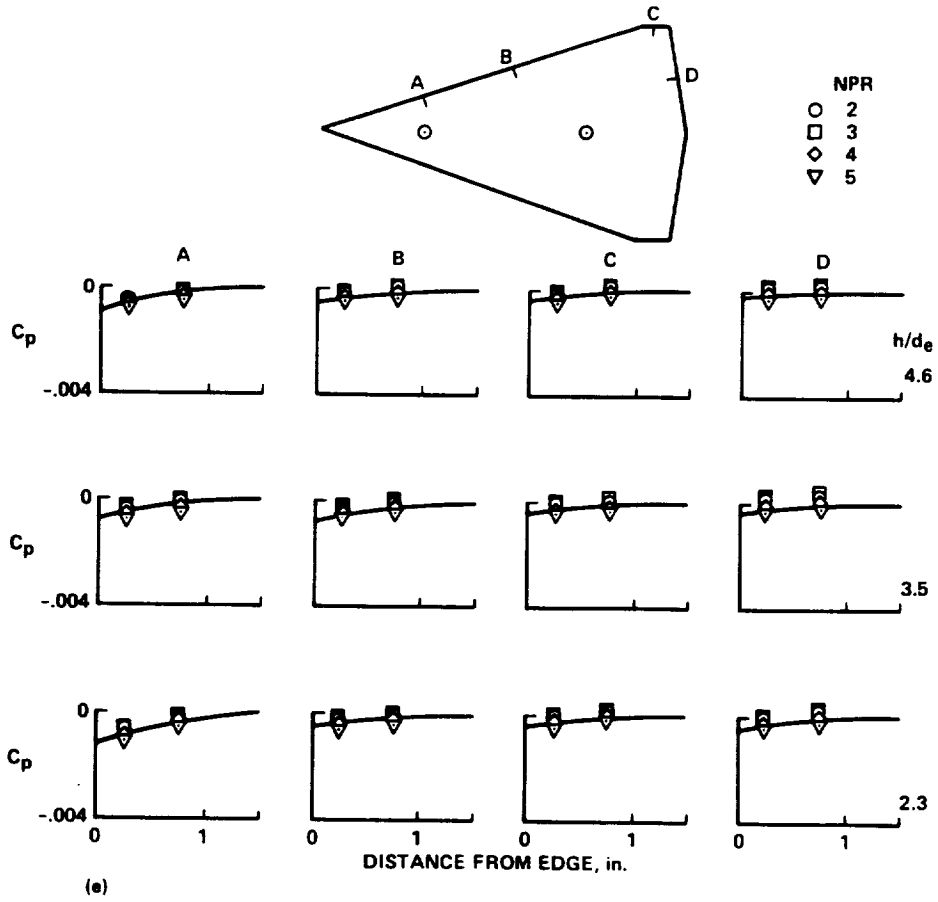

e) Upper surface pressures.

Figure 5. Concluded.

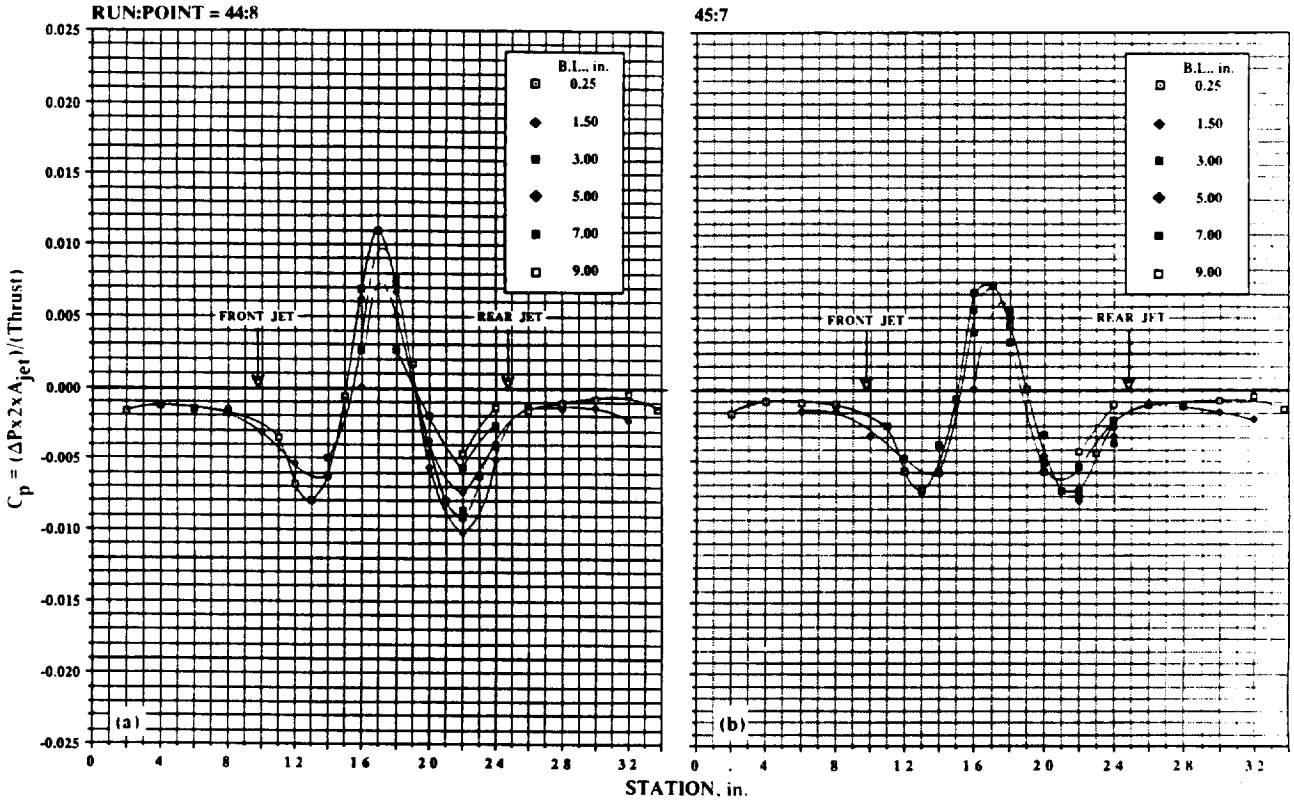

Figure 6. Typical pressure distribution data from the wing-body configuration of reference 4. h/de = 3.5. a) Lower surface pressures, NPR = 2. b) Lower surface pressures, NPR = 4.

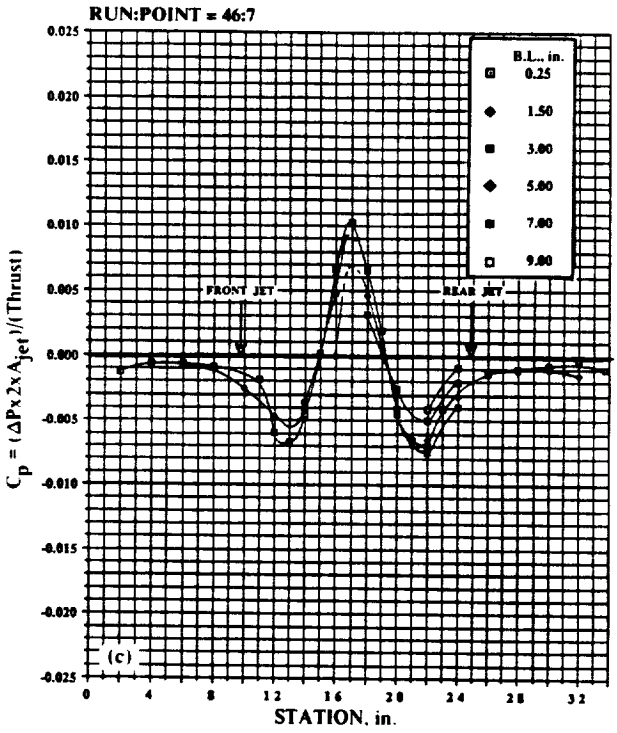

c) Lower surface pressures, NPR = 6.

Figure 6. Continued.

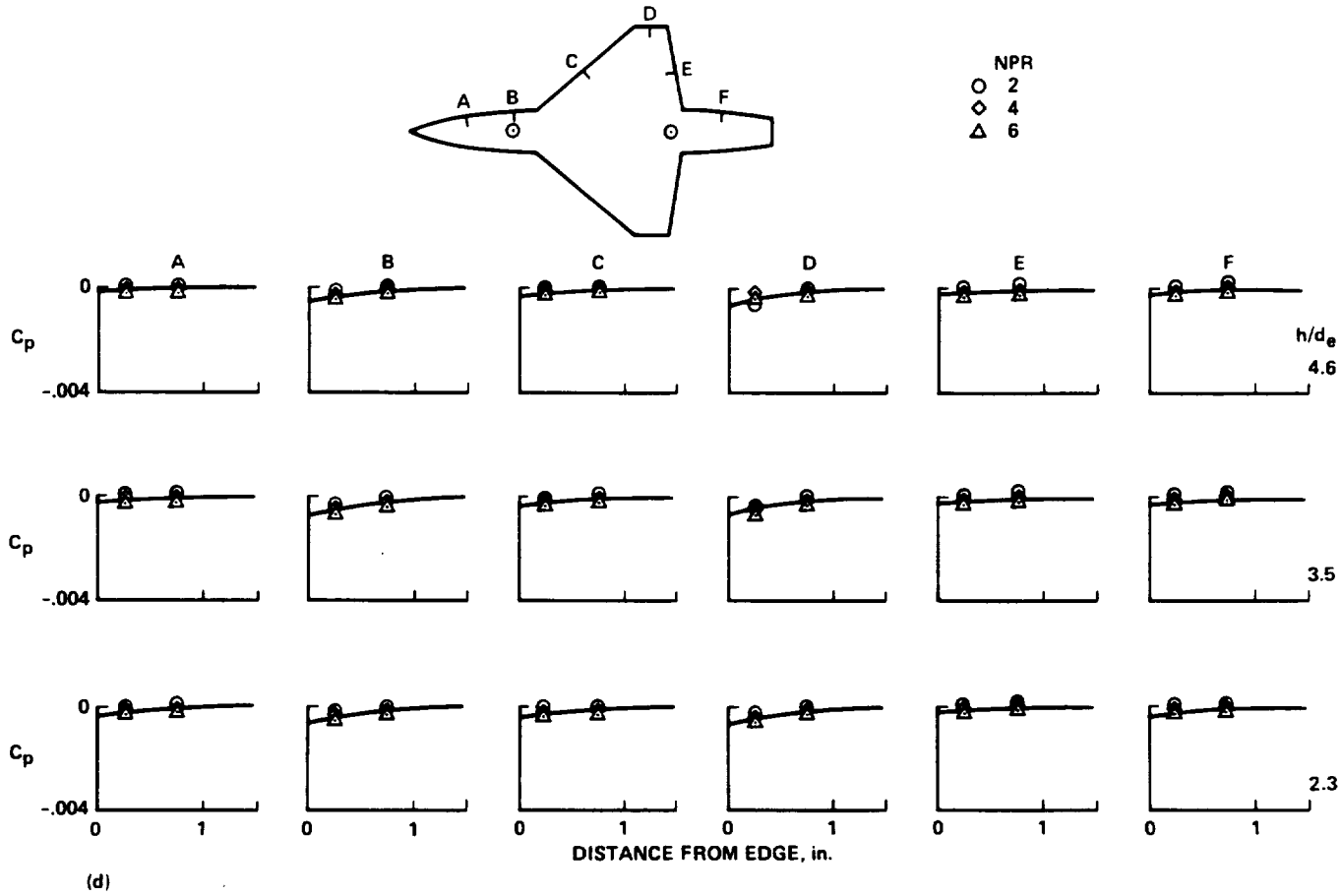

d) Upper surface pressures.

Figure 6. Concluded.

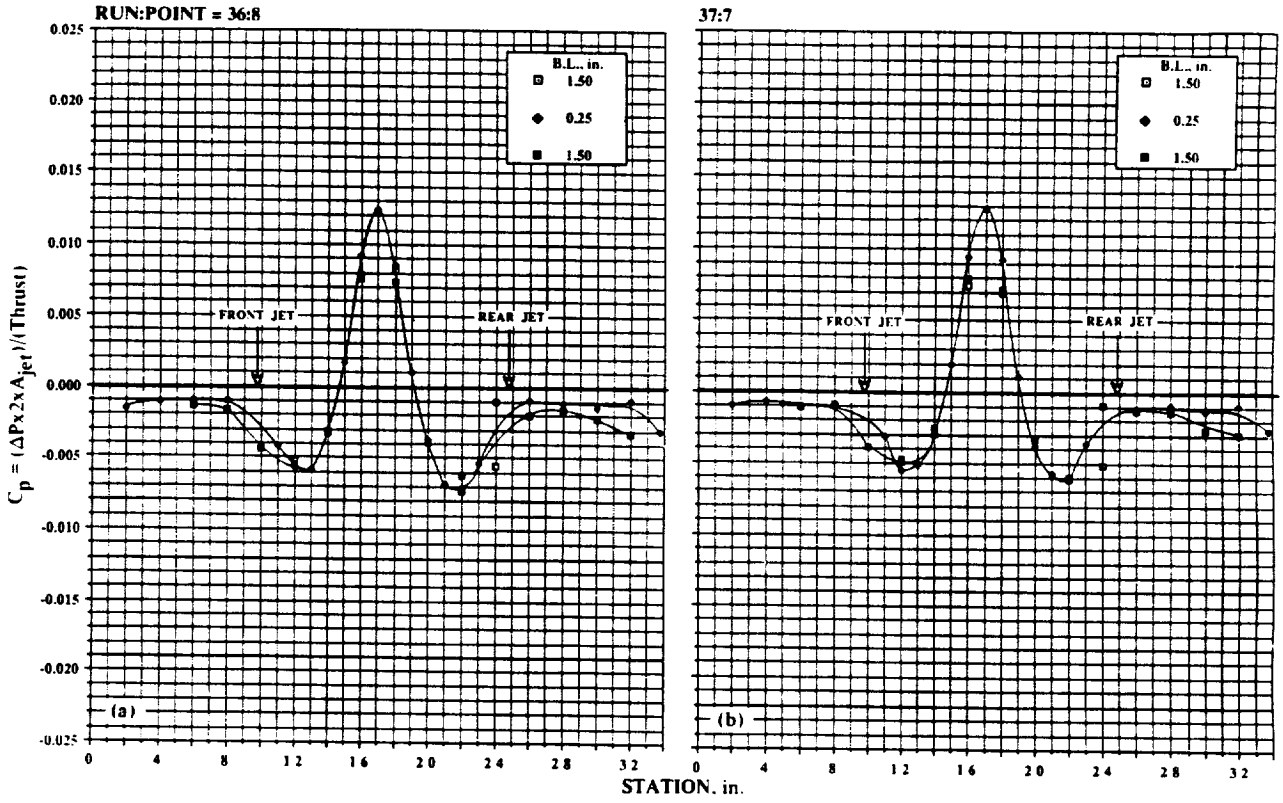

Figure 7. Typical pressure distribution data from the body alone configuration of reference 4. h/de = 3.5. a) Lower surface pressures, NPR = 2. b) Lower surface pressures, NPR = 4.

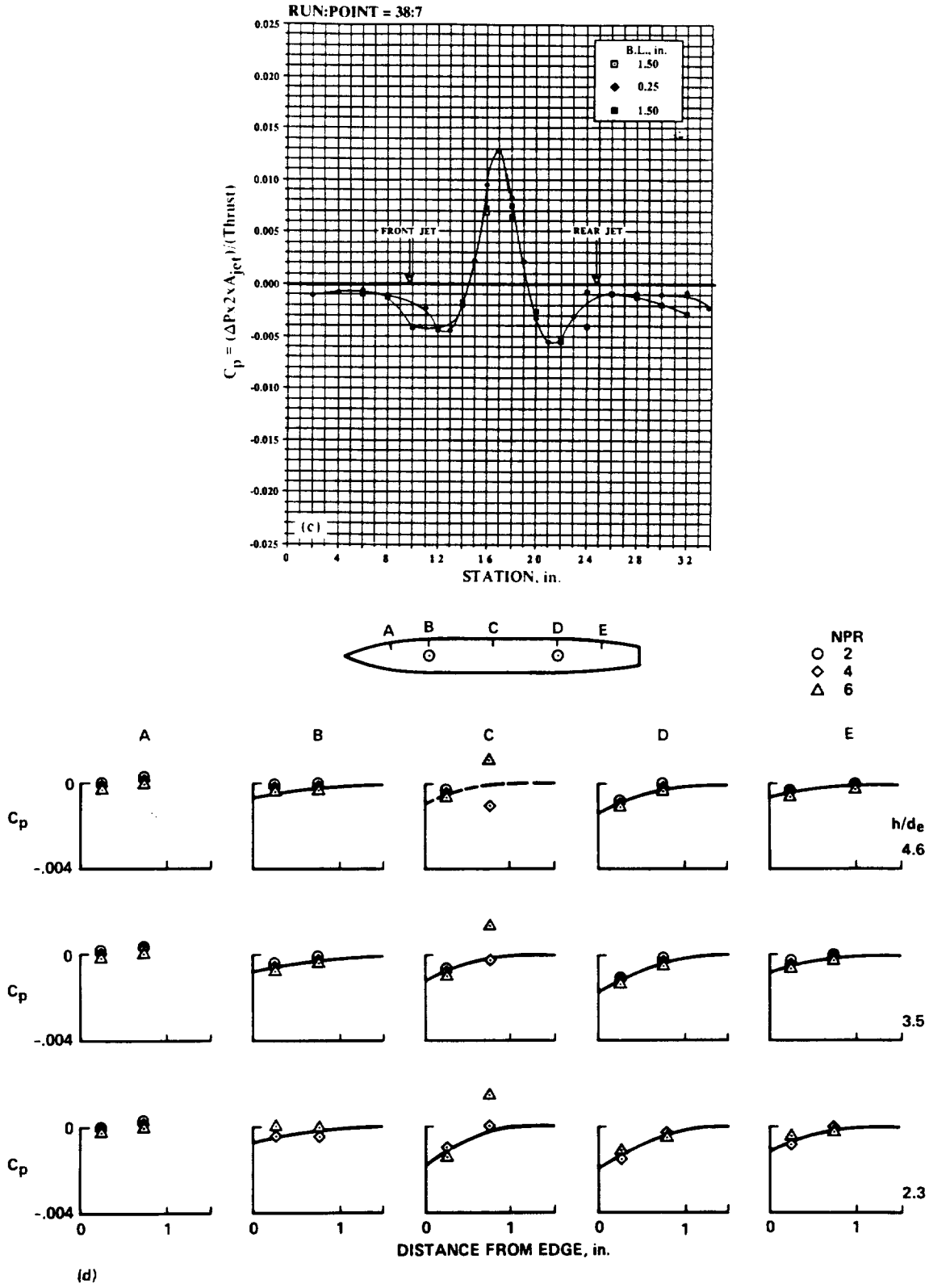

c) Lower surface pressures, NPR = 6. d) Upper surface pressures.

Figure 7. Concluded.

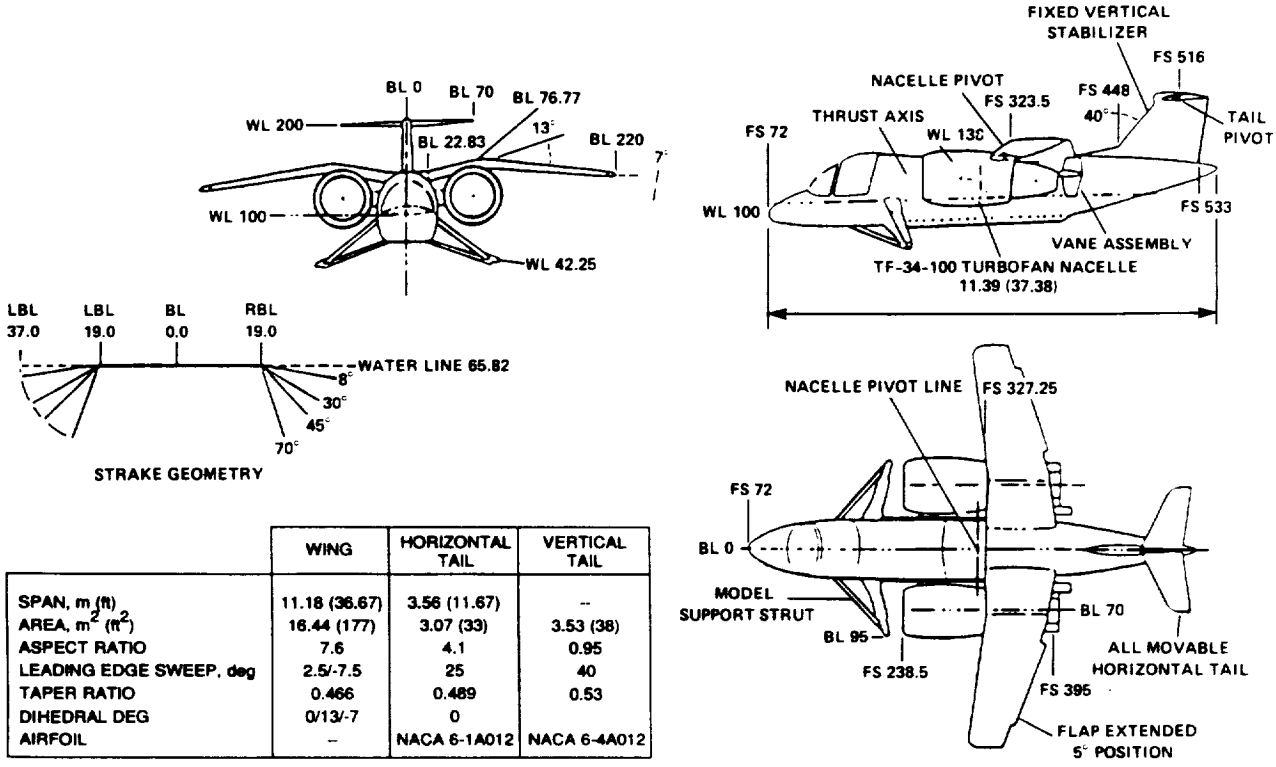

	WING	HORIZONTAL TAIL	VERTICAL TAIL
SPAN, m (ft)	11.18 (36.67)	3.56 (11.67)	--
AREA, m^2 (ft^2)	16.44 (177)	3.07 (33)	3.53 (38)
ASPECT RATIO	7.6	4.1	0.95
LEADING EDGE SWEEP, deg	2.5/-7.5	25	40
TAPER RATIO	0.466	0.489	0.53
DIHEDRAL DEG	0/13/-7	0	
AIRFOIL	--	NACA 6-1A012	NACA 6-4A012

(a) Configuration

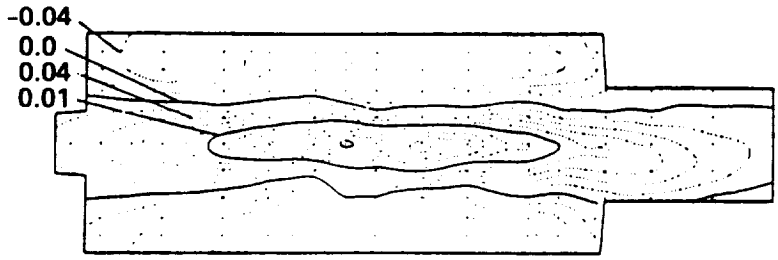

(b) h/de = 0.72

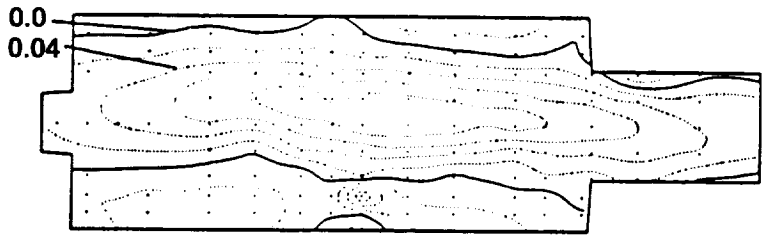

(c) h/de = 1.44

Figure 8. Configuration and typical pressure distribution data from reference 9. a) Configuration. b) h/de = 0.72. c) h/de = 1.44.

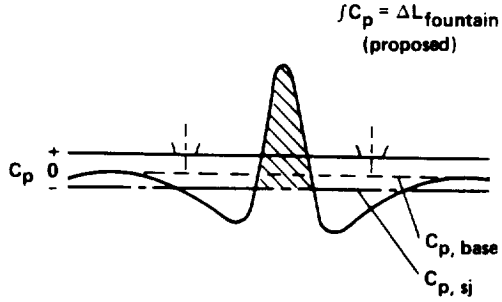

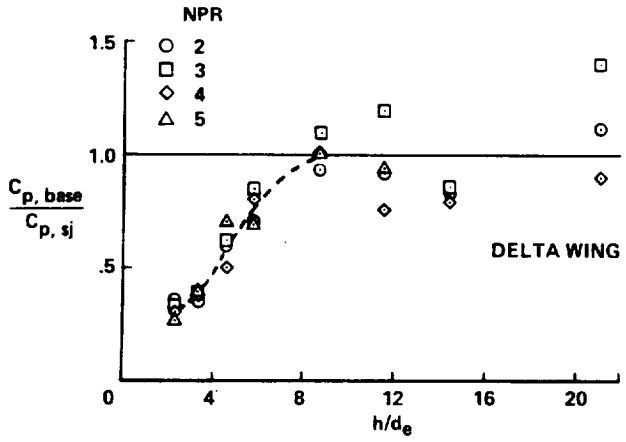

Figure 9. Relation of the pressures induced in the outer regions to the pressures estimated for an equivalent single jet. Delta-wing configuration of reference 4.

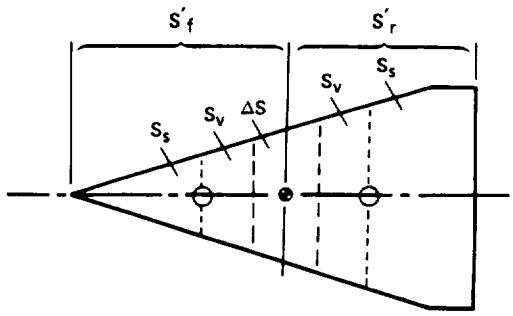

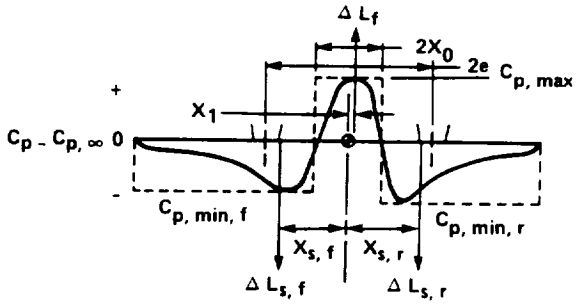

$$\frac{\Delta L}{T} = \frac{\Delta L_\infty}{T} + \frac{\Delta L_f}{T} + \frac{\Delta L_{s,\ f}}{T} + \frac{\Delta L_{s,\ r}}{T}$$

$$\frac{\Delta M}{Td_e} = \frac{\Delta L_\infty}{T}\frac{X_\infty}{d_e} + \frac{\Delta L_f}{T}\frac{X_1}{d_e} + \frac{\Delta L_{s,\ f}}{T}\frac{X_{s,\ f}}{d_e} + \frac{\Delta L_{s,\ r}}{T}\frac{X_{s,\ r}}{d_e}$$

$$\frac{\Delta L_\infty}{T} = K_\infty \sqrt{\frac{S}{A_j}} \left(\frac{\Sigma \pi d}{d_e}\right)^{1.58} (NPR)^{-0.5}$$

$$\frac{\Delta L_f}{T} = K_f \frac{\Delta S}{2A_j} C_{p,\ max}$$

$$\frac{\Delta L_s}{T} = K_s \frac{(S' - \Delta S/2)}{2A_j} (C_{p,\ min} - C_{p,\infty})$$

Figure 10. Presentation of method.

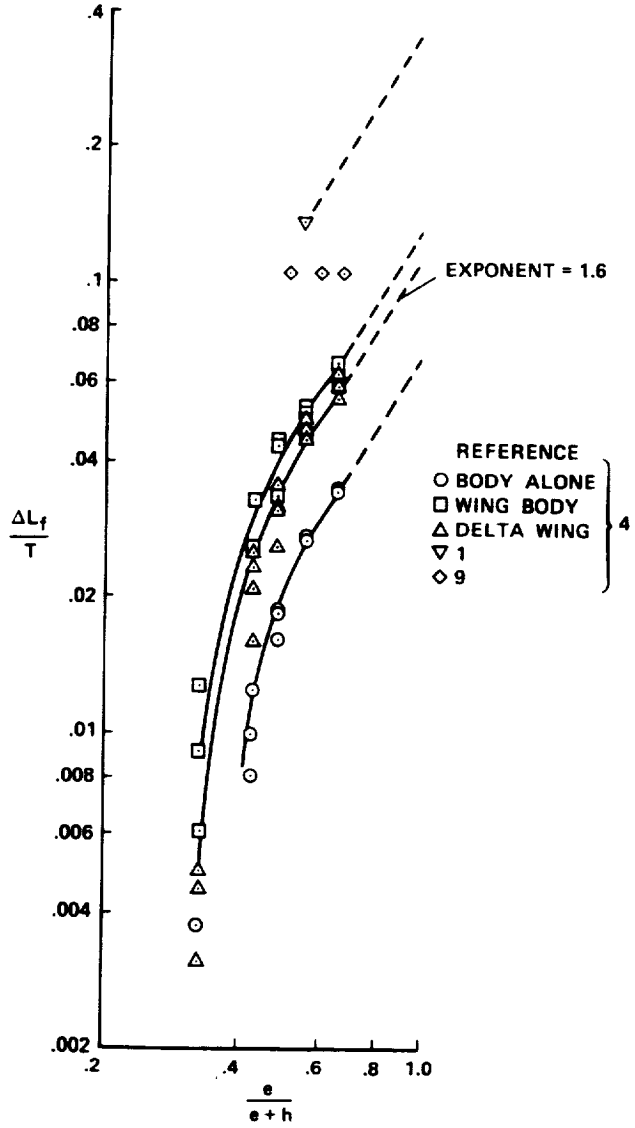

Figure 11. Variation of fountain lift increment with Yen's height parameter.

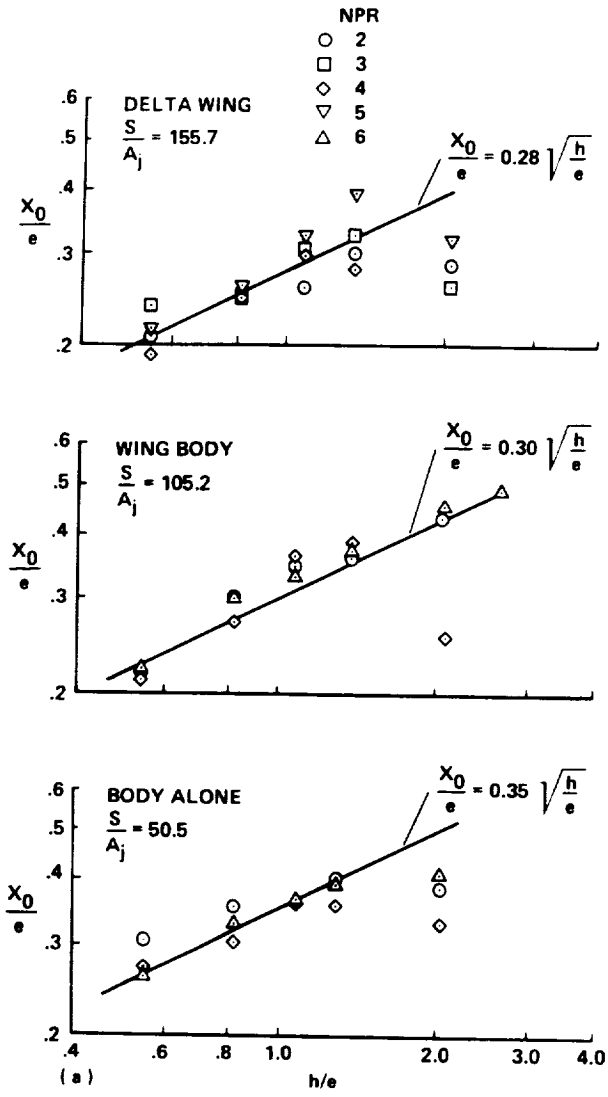

a) Data from reference 4.

Figure 12. Width of fountain region.

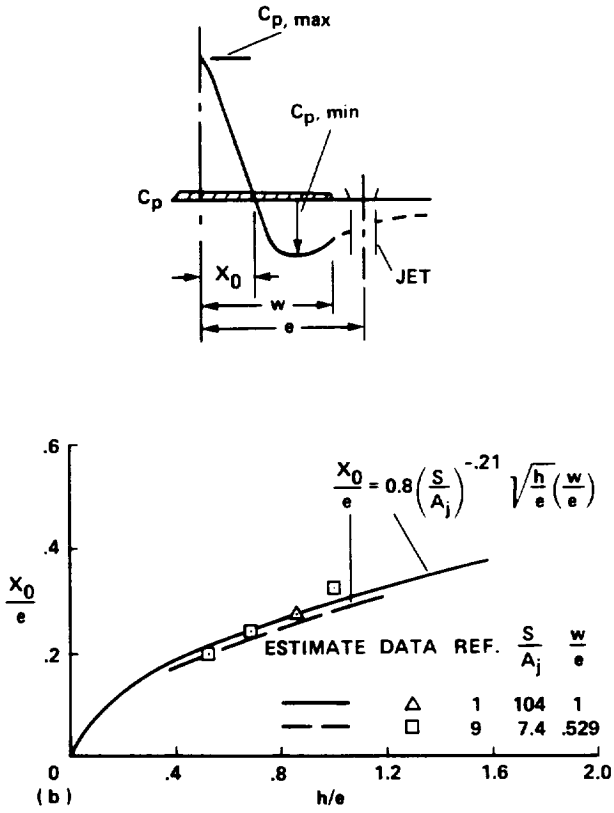

b) Data from references 1 and 9 and definition of terms.

Figure 12. Concluded.

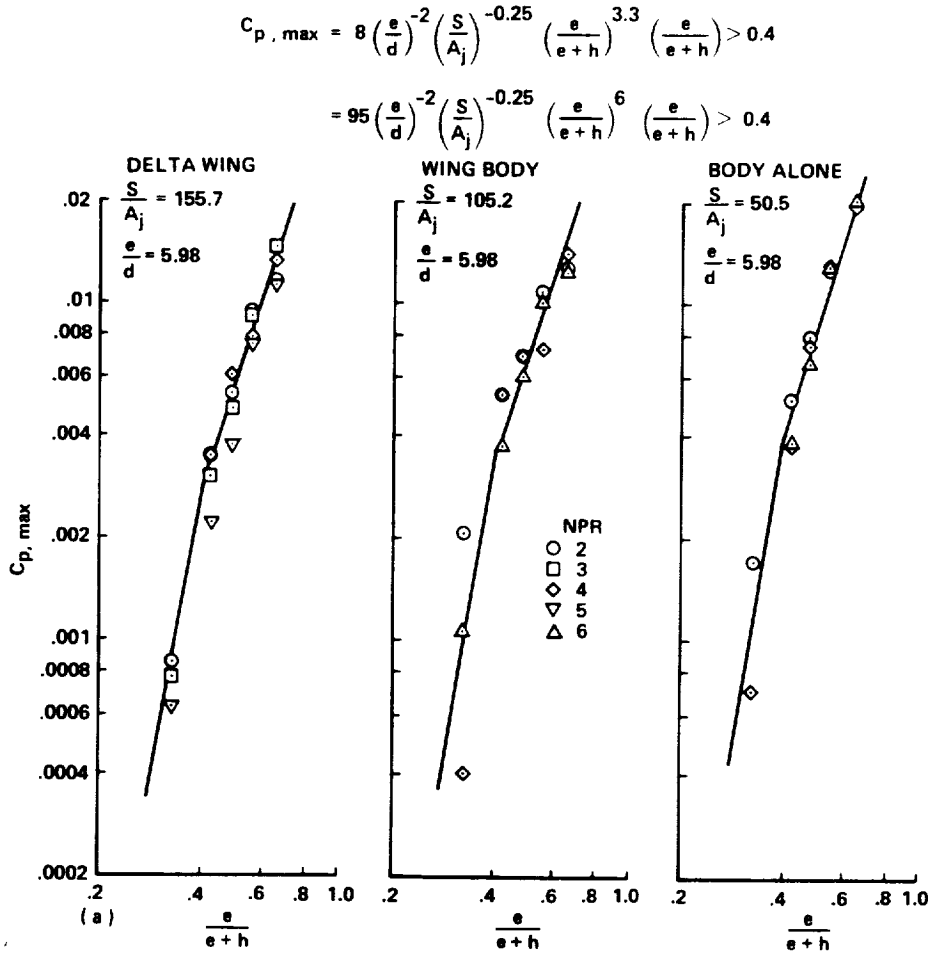

a) Data from reference 4.

Figure 13. Variation of maximum fountain impingement pressure with Yen's height parameter.

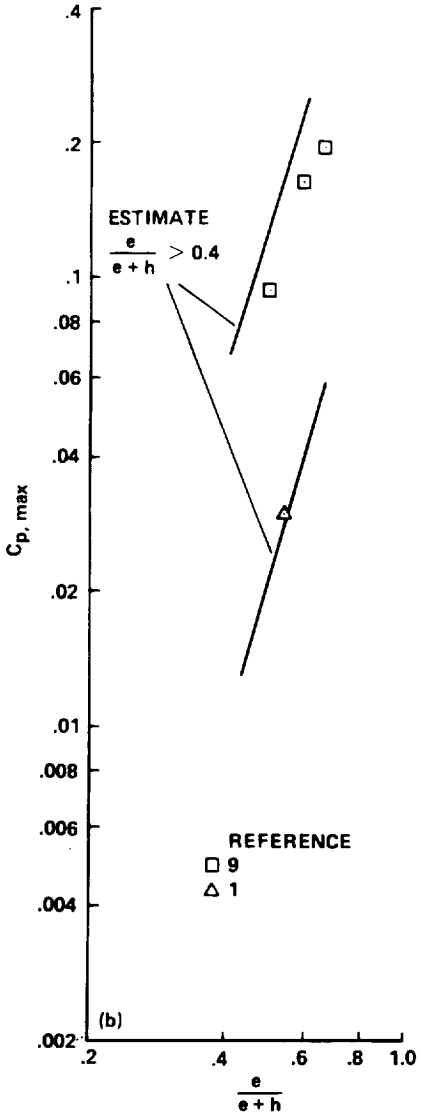

b) Data from reference 1 and 9.

Figure 13. Concluded.

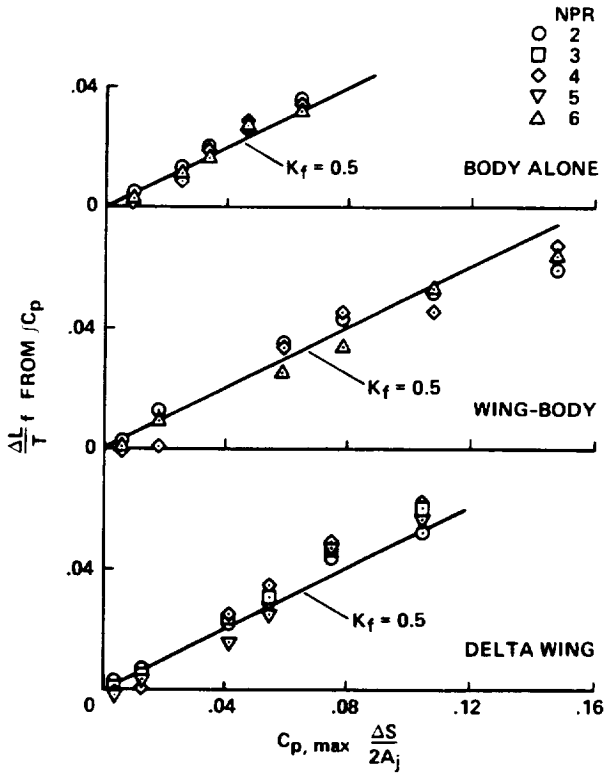

Figure 14. Evaluation of fountain factor K_f.

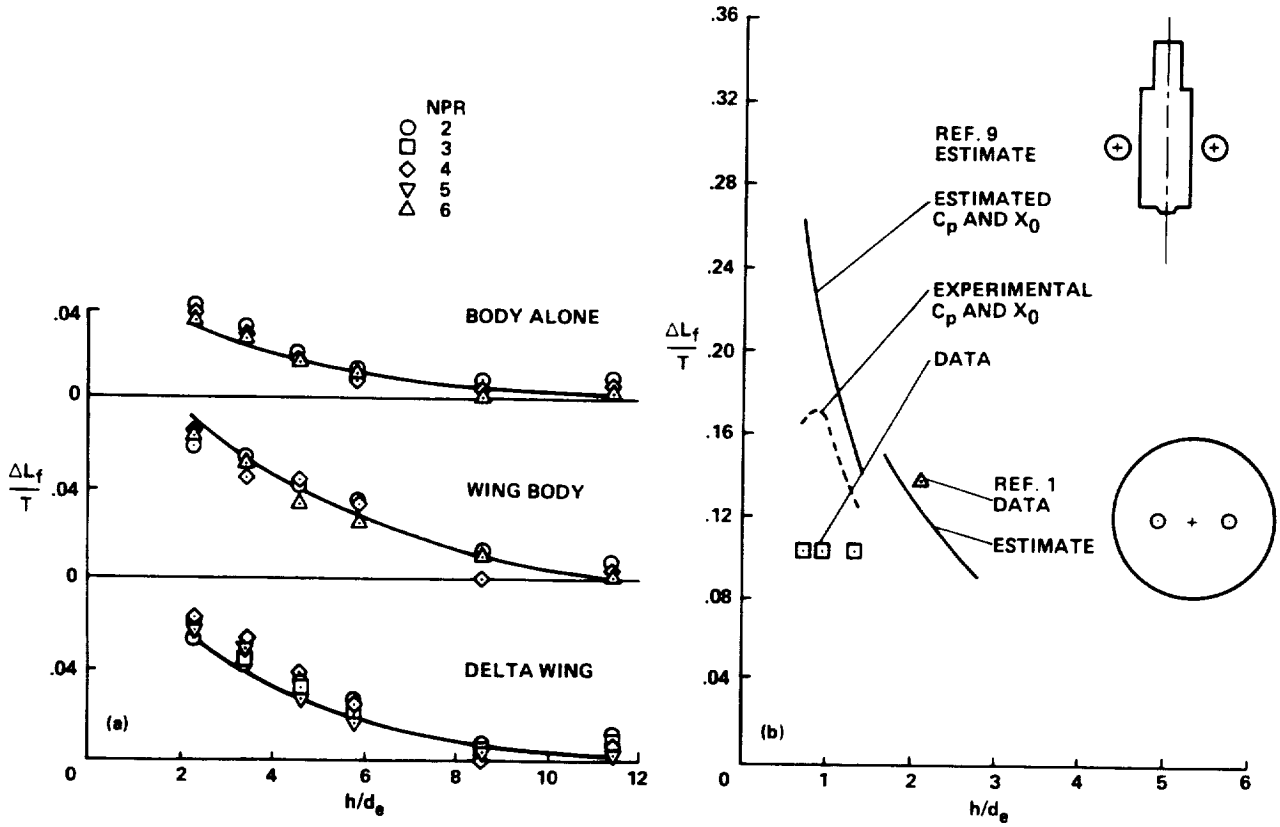

Figure 15. Comparison of estimated fountain lift with experimental data. a) Data from reference 4. b) Data from references 1 and 9.

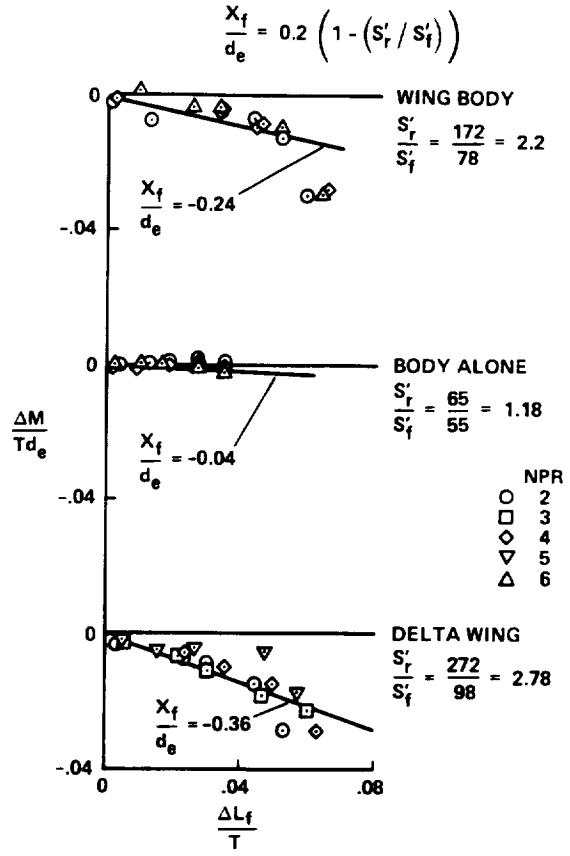

Figure 16. Determination of effective center of fountain lift.

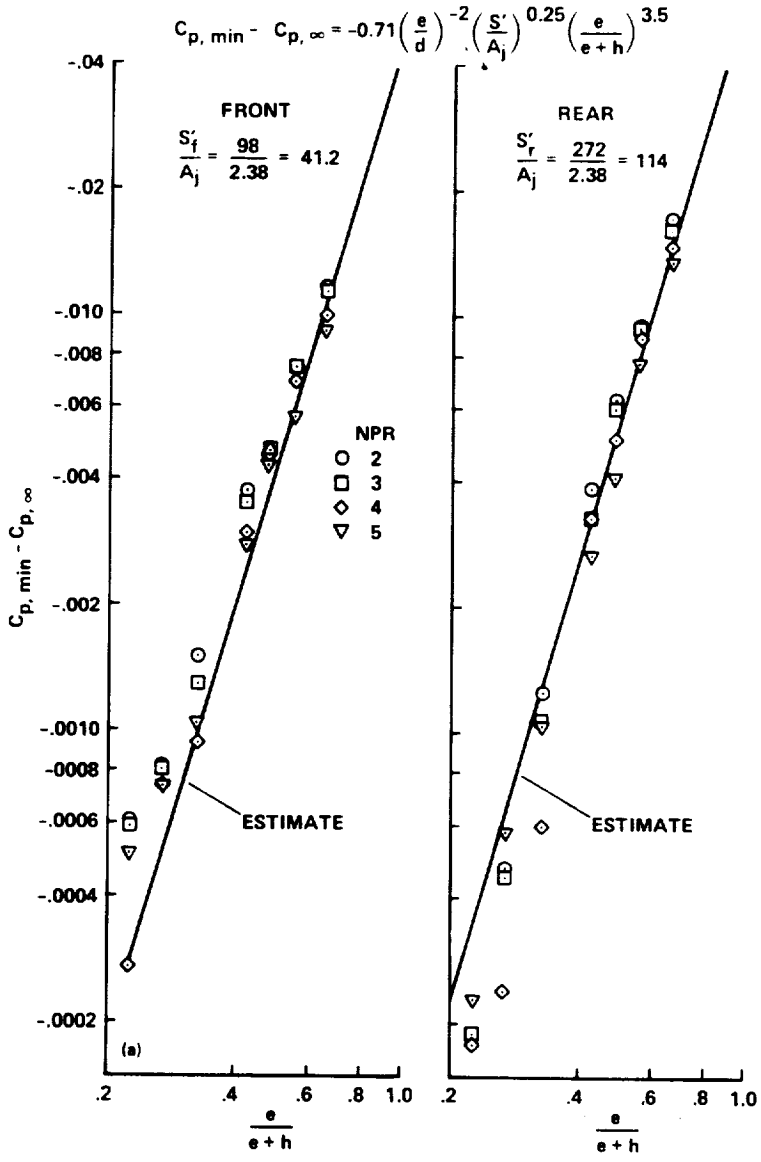

a) Delta-wing configuration of reference 4.

Figure 17. Maximum negative pressure in suckdown region.

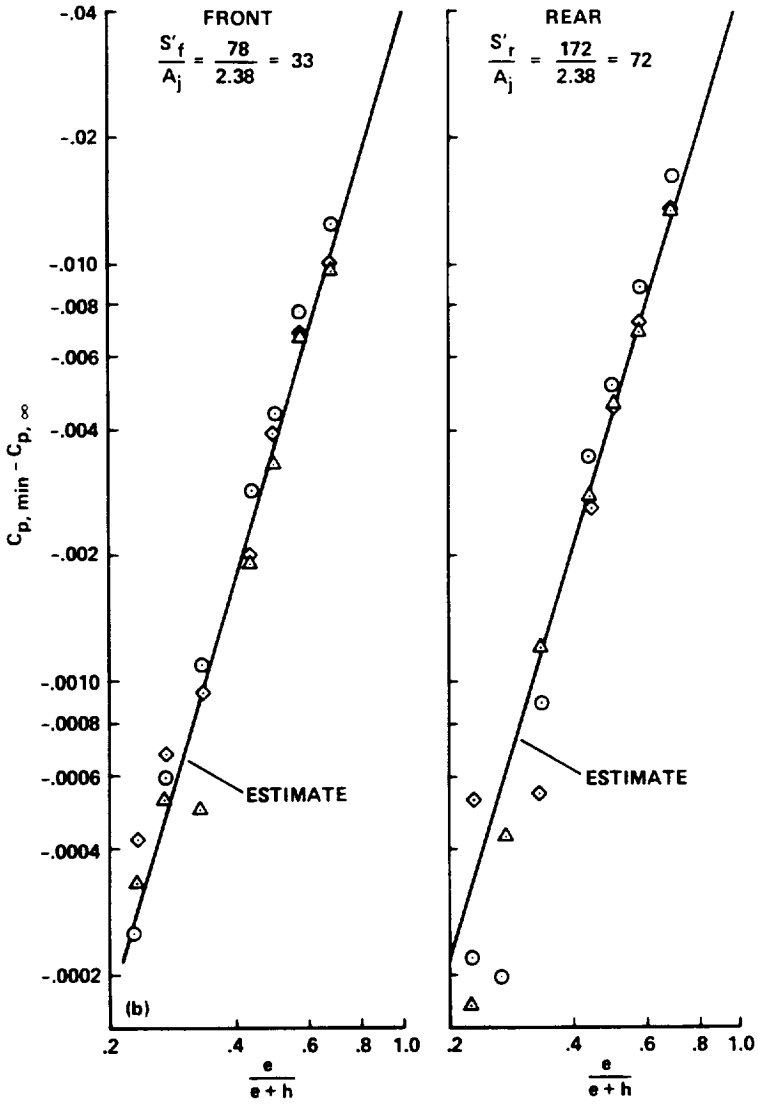

b) Wing-body configuration of reference 4.

Figure 17. Continued.

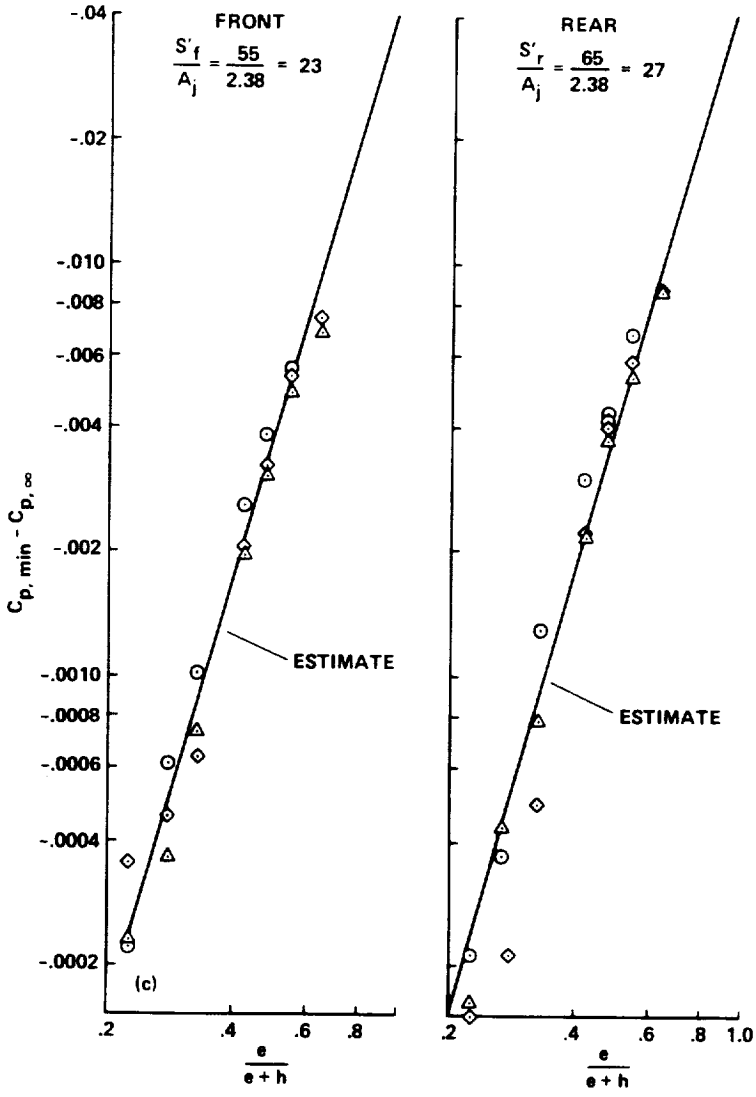

c) Body-alone configuration of reference 4.

Figure 17. Continued.

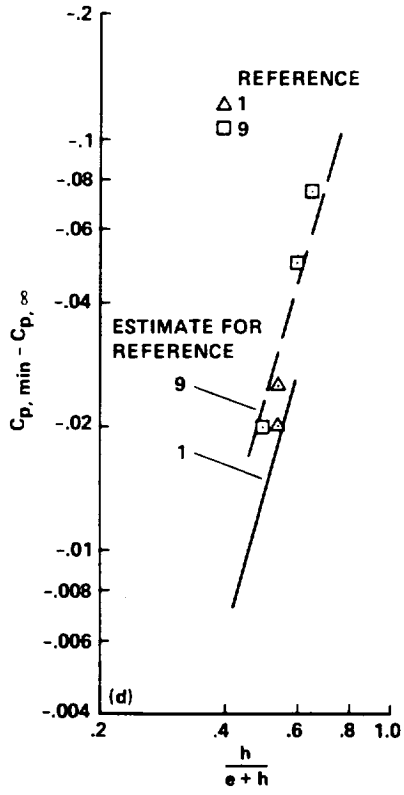

d) Configurations of references 1 and 9.

Figure 17. Concluded.

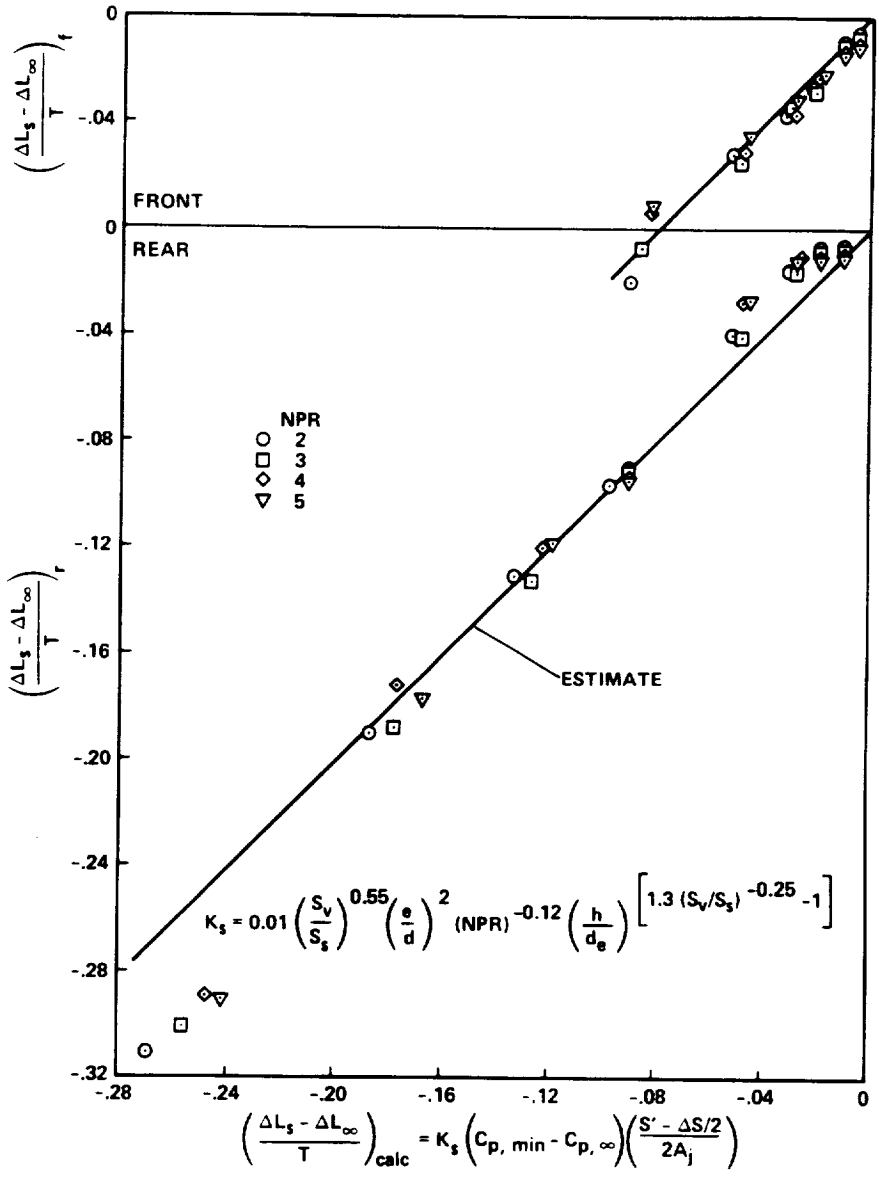

a) Delta-wing configuration of reference 4.

Figure 18. Comparison of calculated suckdown increments with experimental data.

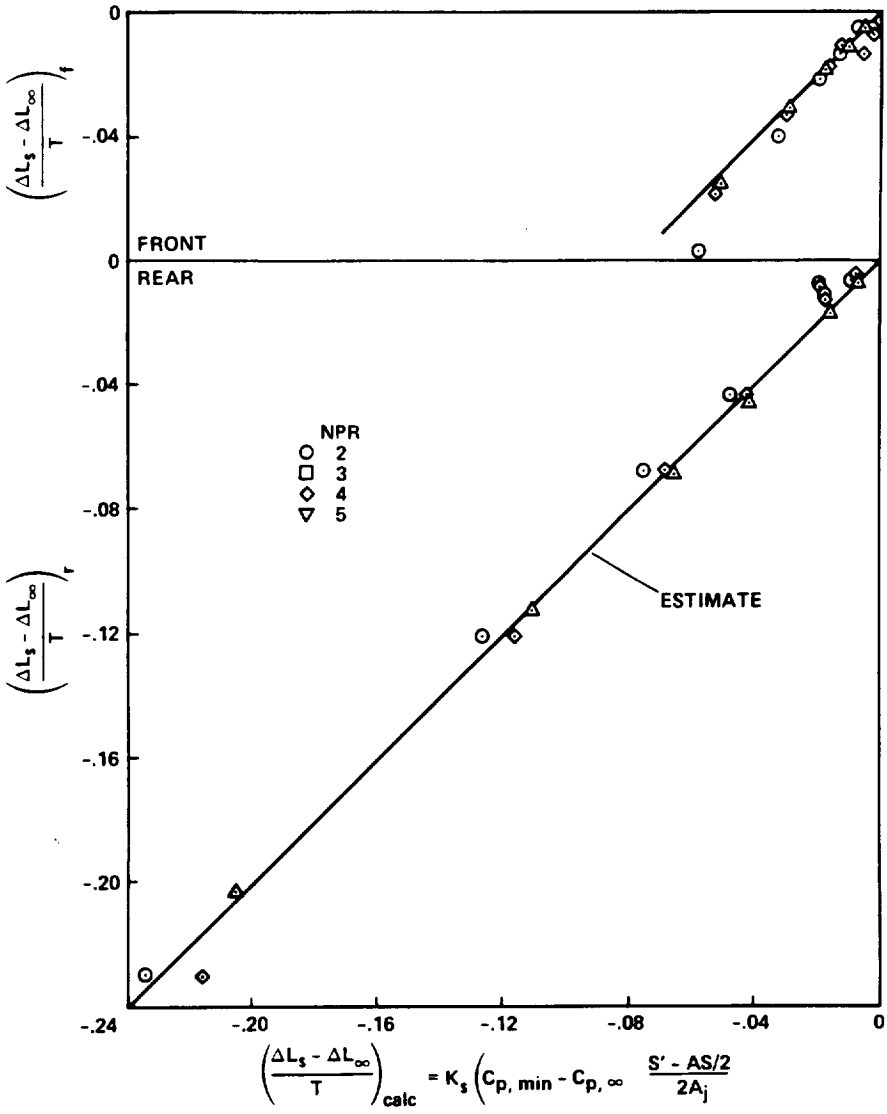

b) Wing-body configuration of reference 4.

Figure 18. Continued.

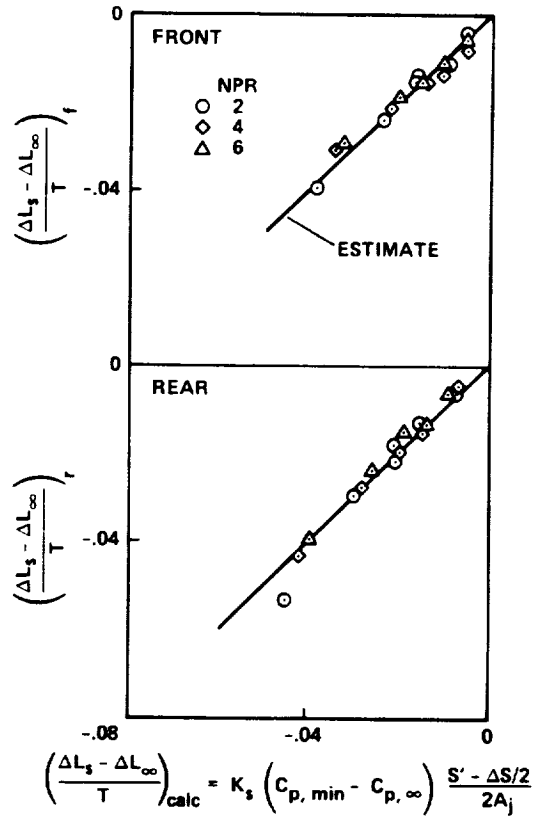

c) Body alone configuration of reference 4.

Figure 18. Concluded.

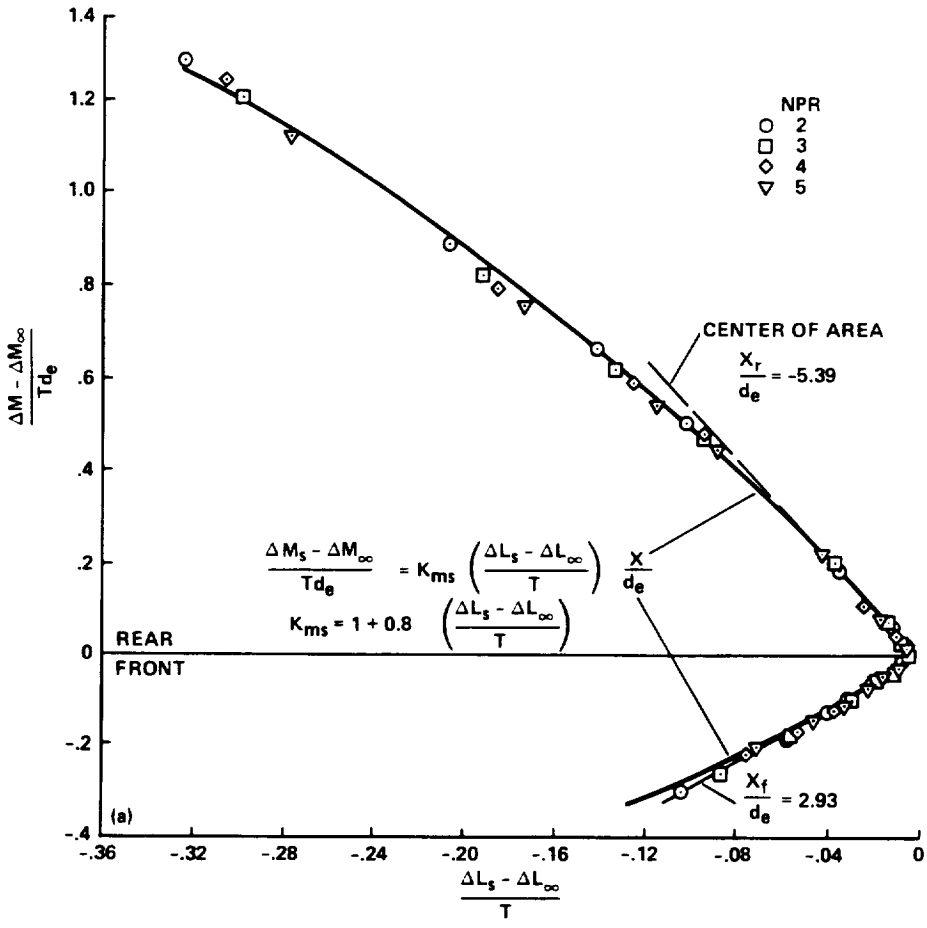

a) Delta-wing configuration of reference 4.

Figure 19. Correlation of pitching moment increments induced on forward and aft suckdown regions.

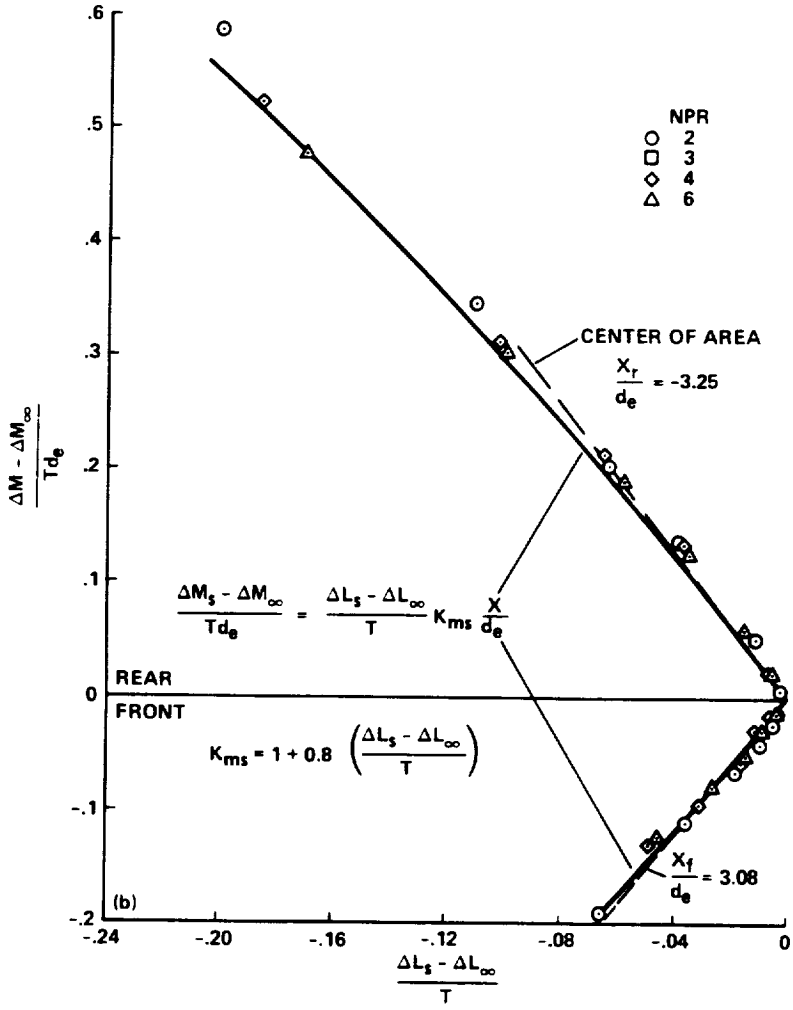

b) Wing-body configuration of reference 4.

Figure 19. Continued.

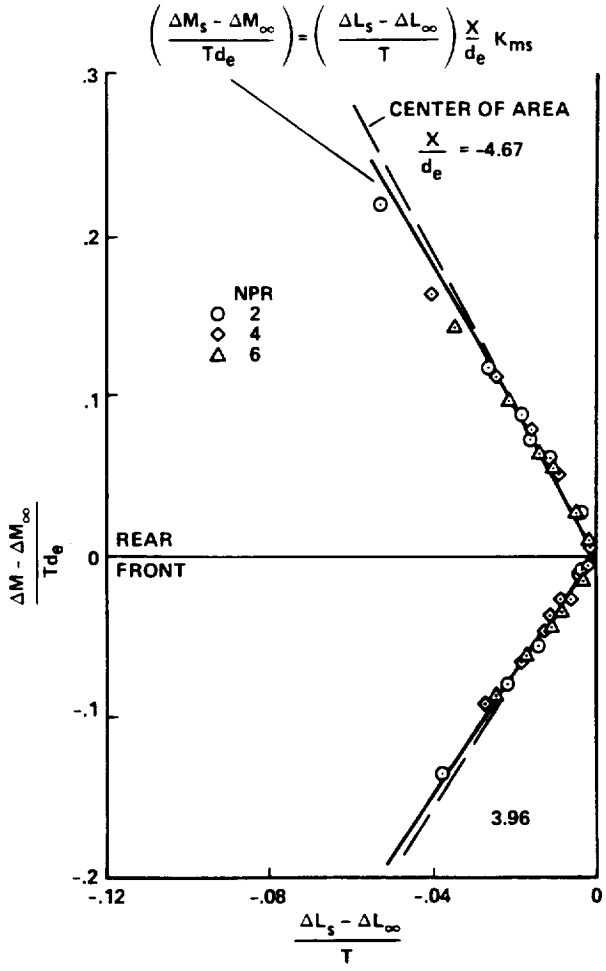

c) Body-alone configuration of reference 4.

Figure 19. Concluded.

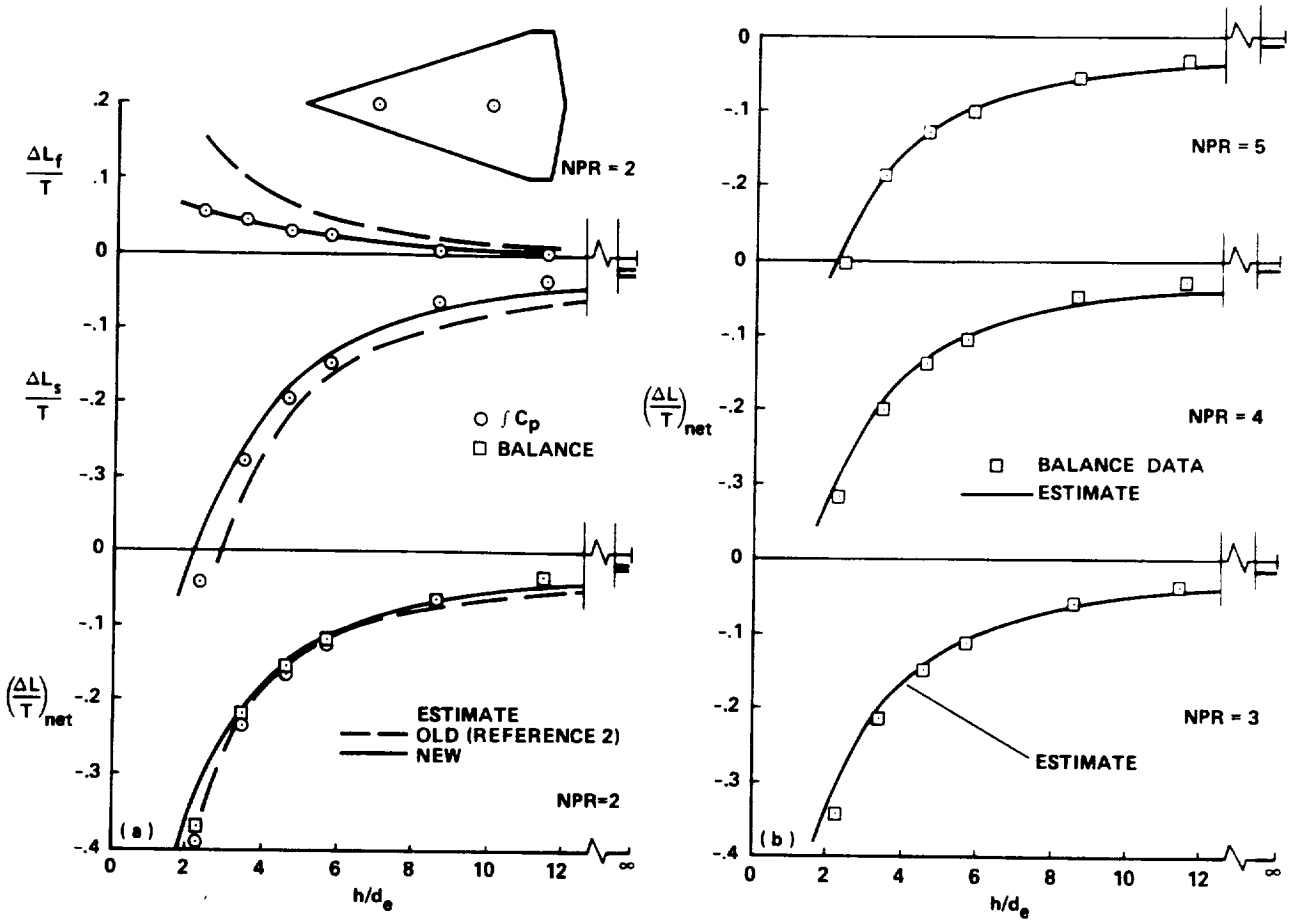

Figure 20. Comparison of estimates with data for delta-wing configuration of reference 4. a) Lift increments, NPR = 2. b) Effect of nozzle pressure ratio on net lift.

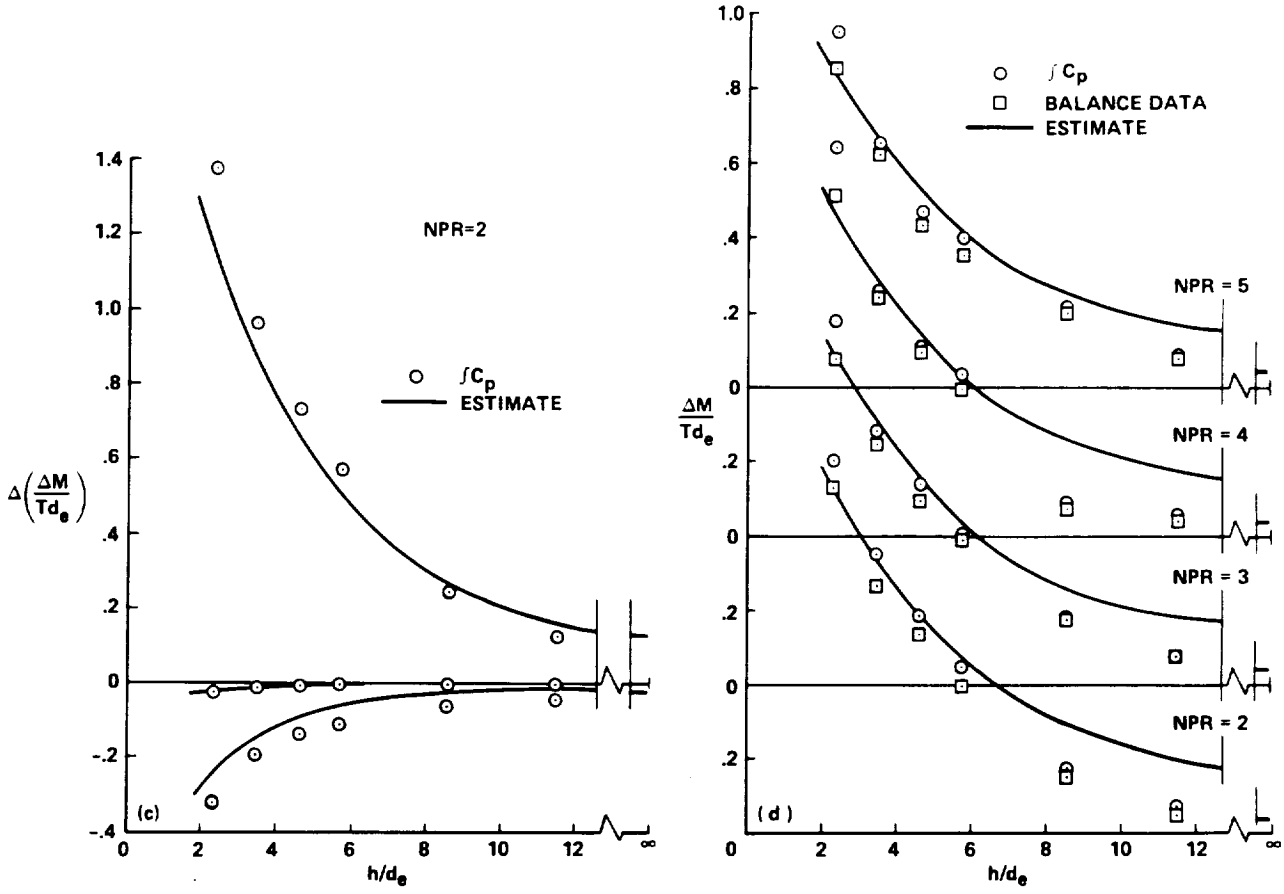

c) Pitching moment increments, NPR = 2. d) Effect of nozzle pressure ratio on moments.

Figure 20. Concluded.

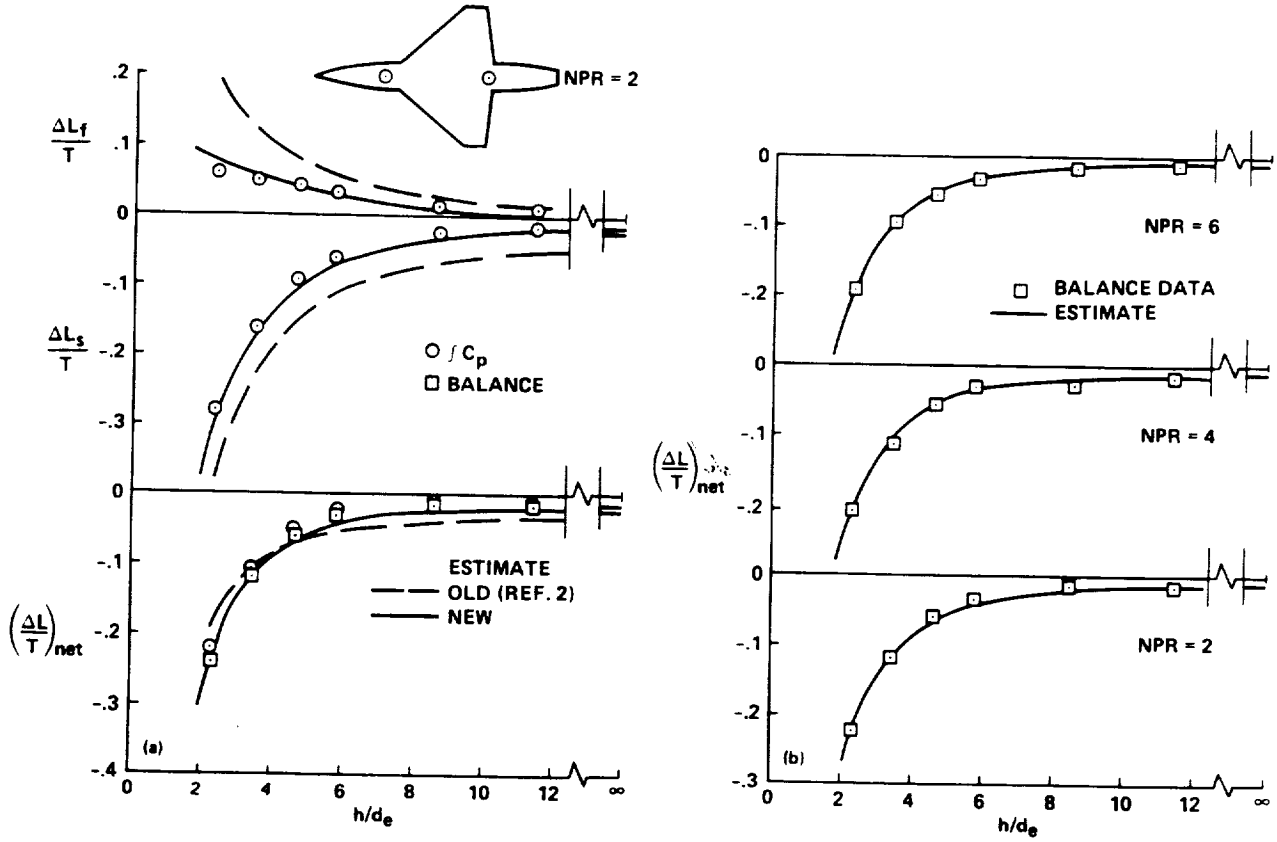

a) Lift increments, NPR = 2. b) Effect of nozzle pressure ratio on net lift.

Figure 21. Comparison of estimates with data for wing-body configuration of reference 4.

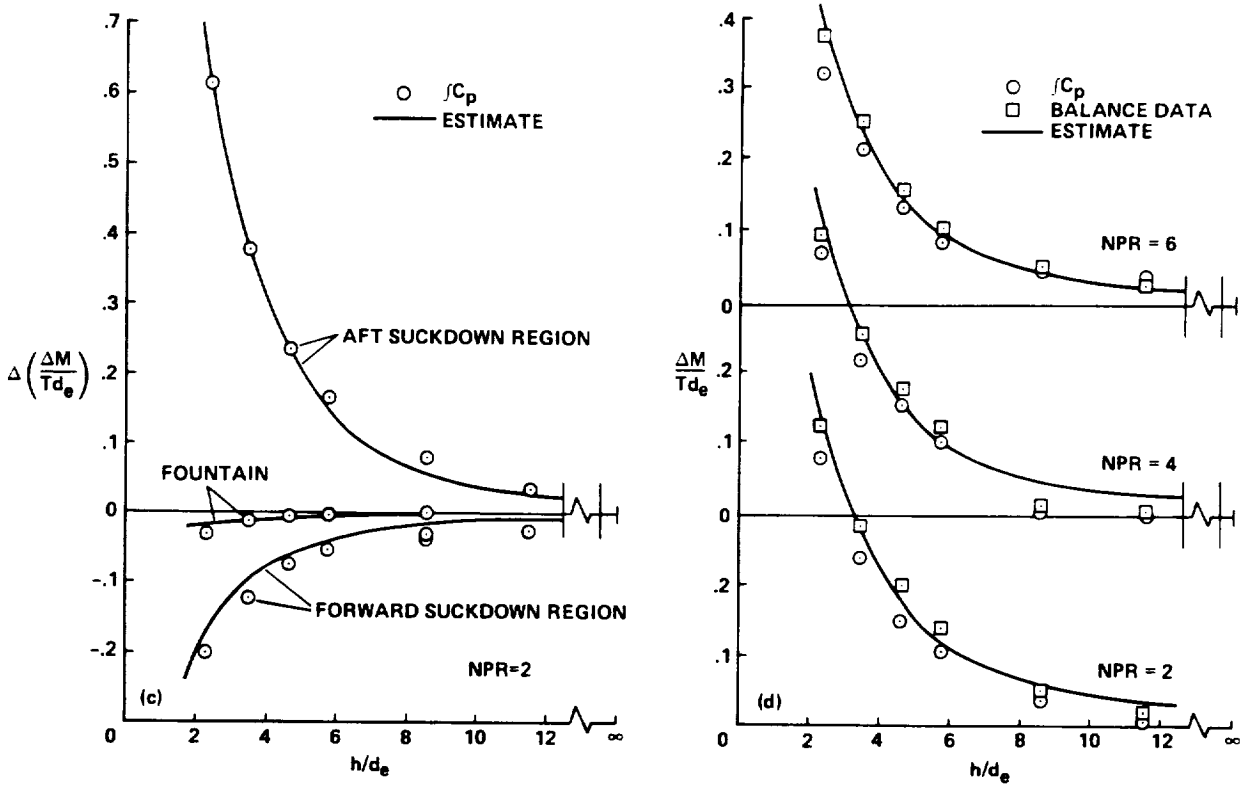

c) Pitching moment increments. d) Effect of nozzle pressure ratio on moments.

Figure 21. Concluded.

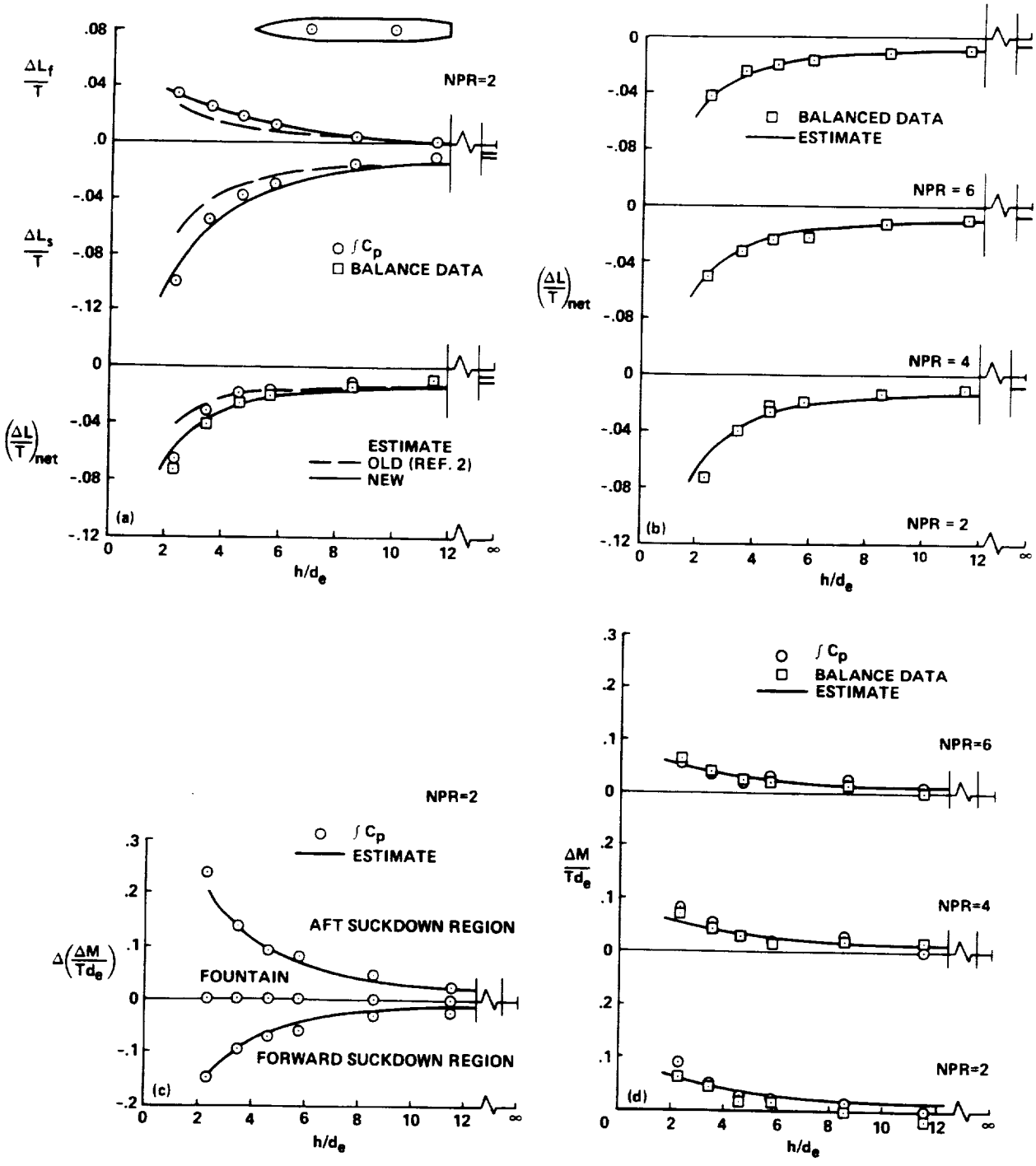

a) Lift increments, NPR = 2. b) Effect of nozzle pressure ratio on lift. c) Pitching moment increments. d) Effect of nozzle pressure ratio on moments.

Figure 22. Comparison of estimates with data for body-alone configuration of reference 4.

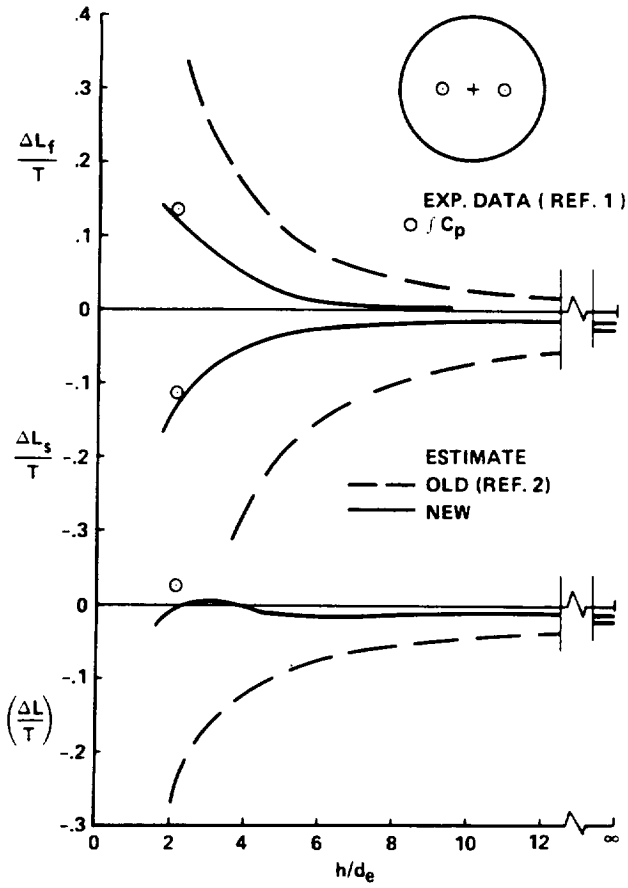

Figure 23. Comparison of estimates with lift data for configuration of reference 1.

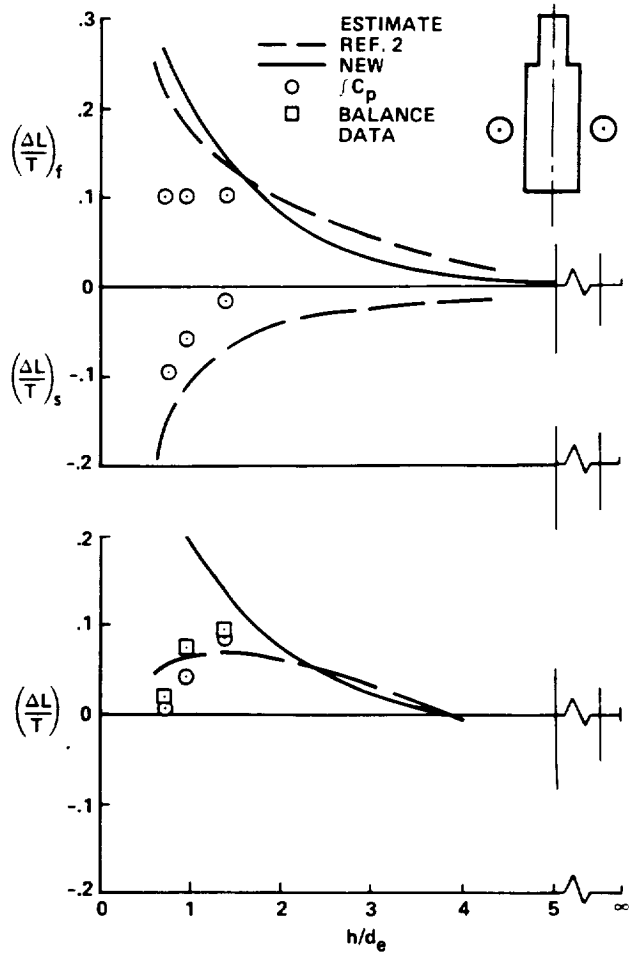

Figure 24. Comparison of estimates with lift data from configuration of reference 9.

REPORT DOCUMENTATION PAGE

Form Approved
OMB No. 0704-0188

1. AGENCY USE ONLY *(Leave blank)*	2. REPORT DATE	3. REPORT TYPE AND DATES COVERED
	August 1991	Technical Memorandum-Final

4. TITLE AND SUBTITLE

On the Estimation of Jet-Induced Fountain Lift and Additional Suckdown in Hover for Two-Jet Configurations

5. FUNDING NUMBERS

505-61-71

6. AUTHOR(S)

Richard E. Kuhn,* David C. Bellavia, Victor R. Corsiglia, and Douglas A. Wardwell

7. PERFORMING ORGANIZATION NAME(S) AND ADDRESS(ES)

Ames Research Center
Moffett Field, CA 94035-1000

8. PERFORMING ORGANIZATION REPORT NUMBER

A-90040

9. SPONSORING/MONITORING AGENCY NAME(S) AND ADDRESS(ES)

National Aeronautics and Space Administration
Washington, DC 20546-0001

10. SPONSORING/MONITORING AGENCY REPORT NUMBER

NASA TM-102268

11. SUPPLEMENTARY NOTES

Point of Contact: Douglas A. Wardwell, Ames Research Center, MS 237-3, Moffett Field, CA 94035-1000; (415) 604-6566 or FTS 464-6566
*STO-VL Technology, San Diego, California

12a. DISTRIBUTION/AVAILABILITY STATEMENT

Unclassified — Unlimited
Subject Category 02

12b. DISTRIBUTION CODE

13. ABSTRACT *(Maximum 200 words)*

Currently available methods for estimating the net suckdown induced on jet V/STOL aircraft hovering in ground effect are based on a correlation of available force data and are therefore limited to configurations similar to those in the data base. Experience with some of these configurations has shown that both the fountain lift and additional suckdown are overestimated but these effects cancel each other for configurations within the data base. For other configurations these effects may not cancel and the net suckdown could be grossly overestimated or underestimated. Also, present methods do not include the prediction of the pitching moments associated with the suckdown induced in ground effect.

The present study begins an attempt to develop a more logically based method for estimating the fountain lift and suckdown based on the jet-induced pressures. The present analysis is based primarily on the data from a related family of three two-jet configurations (all using the same jet spacing) and limited data from two other two-jet configurations.

This report presents the current status of the method, which includes expressions for estimating the maximum pressure induced in the fountain region, the minimum pressures induced in the suckdown regions, and the sizes of the fountain and suckdown regions. Correlating factors are developed to be used with these areas and pressures to estimate the fountain lift, the suckdown, and the related pitching moment increments.

14. SUBJECT TERMS

Propulsion-induced aerodynamics, STOVL aircraft, VTOL aircraft, Lift loss, Fountain lift, Pitching moment

15. NUMBER OF PAGES

53

16. PRICE CODE

A04

17. SECURITY CLASSIFICATION OF REPORT	18. SECURITY CLASSIFICATION OF THIS PAGE	19. SECURITY CLASSIFICATION OF ABSTRACT	20. LIMITATION OF ABSTRACT
Unclassified	Unclassified		